

Risk-Sensitive Diffusion for Perturbation-Robust Optimization

Yangming Li*, Max Ruiz Luyten, Mihaela van der Schaar

Department of Applied Mathematics and Theoretical Physics
University of Cambridge

Abstract

The essence of score-based generative models (SGM) is to optimize a score-based model $\mathbf{s}_\theta(\mathbf{x}, t)$ towards the score function $\nabla_{\mathbf{x}} \ln p_t(\mathbf{x})$. However, we show that noisy samples incur another objective function, rather than the one with score function, which will wrongly optimize the model. To address this problem, we first consider a new setting where every noisy sample is paired with a *risk vector* \mathbf{r} , indicating the data quality (e.g., noise level). This setting is very common in real-world applications, especially for medical and sensor data.

Then, we introduce *risk-sensitive SDE*, a type of stochastic differential equation (SDE) parameterized by the risk vector. With this tool, we aim to minimize a measure called *perturbation instability* $\mathcal{S}_t(\mathbf{r}) \geq 0$, which we define to quantify the negative impact of noisy samples on optimization. We will prove that zero measure: $\mathcal{S}_t(\mathbf{r}) = 0$, is only achievable in the case where noisy samples are caused by Gaussian perturbation. For non-Gaussian cases, we will also provide its optimal coefficients that minimize the misguidance of noisy samples: $\mathcal{S}_t(\mathbf{r})$. To apply risk-sensitive SDE in practice, we extend widely used diffusion models to their risk-sensitive versions and derive a risk-free loss that is efficient for computation.

We also have conducted numerical experiments to confirm the validity of our theorems and show that they let SGM be robust to noisy samples for optimization.

*Email address for contact: y1874@cam.ac.uk.

Contents

1	Introduction	1
1.1	Main Theory	2
1.2	Wide Applications	4
2	Related Work	6
3	Preliminaries	6
3.1	Background of SGM	6
3.2	Problem Formulation	7
3.3	Basic Definitions	8
4	Stability for Gaussian Perturbation	10
4.1	Risk-sensitive Kernel	10
4.2	Solution for Gaussian Perturbation	12
5	Minimum Instability for General Noises	14
5.1	Spectral Representation	14
5.2	Necessary Condition for Achieving Stability	16
5.3	Solution for General Noises	17
6	Applications to SGM	18
6.1	Extensions under Gaussian Perturbation	19
6.2	Optimization and Sampling	20
6.3	Extension under Cauchy Perturbation	23
A	Risk-conditional SGM	30
A.1	Risk as the Variable	30
A.2	Risk as the Conditional	30
B	Backward Risk-sensitive SDE	31
C	Numerical Experiments	32
C.1	Proof-of-concept Experiments	32
C.2	Application Experiments	33

1 Introduction

Score-based generative models (SGM) [SE19, SSDK⁺21] (or diffusion models [SDWVG15, HJA20]) stand as a huge progress in the field of generative models, with state-of-the-art performance in data synthesis [DN21, KPH⁺21, LTG⁺22] and solid mathematical foundation [SSDK⁺21, HLC21]. The core of SGM is the *diffusion process*, which is shaped as a stochastic differential equation (SDE) [Itô44] with predefined coefficients $f(t), g(t)$:

$$d\mathbf{x}(t) = f(t)\mathbf{x}(t)dt + g(t)d\mathbf{w}(t),$$

leading a real sample $\mathbf{x}(0) \in \mathbb{R}^D$ to an approximately Gaussian-distributed noise $\mathbf{x}(T)$. To sample from SGM, this diffusion process is reversed in time as

$$d\mathbf{x}(t) = (f(t)\mathbf{x}(t) - g(t)^2\nabla_{\mathbf{x}(t)} \ln p_t(\mathbf{x}(t)))dt + g(t)d\bar{\mathbf{w}}(t),$$

which transforms a Gaussian noise $\mathbf{x}(T)$ into a real sample $\mathbf{x}(0)$. In this *reversed process*, a commonly inaccessible term $\nabla_{\mathbf{x}} \ln p_t(\mathbf{x})$ is introduced: the score function of distribution $p_t(\mathbf{x})$. Common practices [HJA20, SSDK⁺21] resort to neural networks $\mathbf{s}_\theta(\mathbf{x}, t)$ [LBH15] to approximate the score function, which is also called the score-based model.

In this paper, we are interested in a rarely studied situation, where the observed sample $\mathbf{x}(0)$ to optimize the score-based model $\mathbf{s}_\theta(\mathbf{x}, t)$ might be perturbed with some type of noise and we also have some prior information about the noise distribution: risk vector \mathbf{r} . We will see in Sec. 1.2 that this is very common in real-world applications. For example, sensor data mostly come with information indicating the data quality [SC05]. In terms of vanilla SGM (e.g., DDPM [HJA20]), such a noisy sample $\tilde{\mathbf{x}}(0)$ will lead the score-based model $\mathbf{s}_\theta(\mathbf{x}, t)$ to estimating a biased score function $\nabla_{\mathbf{x}} \ln \tilde{p}_{t,\mathbf{r}}(\mathbf{x}) \neq \nabla_{\mathbf{x}} \ln p_t(\mathbf{x})$. In this sense, the model $\mathbf{s}_\theta(\mathbf{x}, t)$ at every time step t is wrongly optimized and has a non-negligible estimation error, so the reverse process will suffer from error propagation [LvdS24], generating a distributionally shifted sample $\tilde{\mathbf{x}}(0)$.

To robustly optimize the score-based model $\mathbf{s}_\theta(\mathbf{x}, t)$ with noisy sample $(\tilde{\mathbf{x}}(0), \mathbf{r})$, we introduce *risk-sensitive SDE*, a type of SDE with coefficients that are specified by the risk information \mathbf{r} . As a preview, its informal definition is in the following.

Definition 1 (Risk-sensitive SDE, Simplified Version of Definition 4). *For a sample-risk pair $(\tilde{\mathbf{x}}(0), \mathbf{r})$, a risk-sensitive SDE is a SDE that incorporates the risk \mathbf{r} into its coefficients, unfolding the sample $\tilde{\mathbf{x}}(0)$ through $t \in [0, T]$ as*

$$d\tilde{\mathbf{x}}(t) = f(\mathbf{r}, t)\tilde{\mathbf{x}}(t)dt + g(\mathbf{r}, t)d\mathbf{w}(t), \tag{1}$$

where risk-sensitive coefficients $f(\mathbf{r}, t), g(\mathbf{r}, t)$ are extended from the risk-unaware coefficients of a vanilla diffusion process: $f(t), g(t)$, for zero risk $\mathbf{r} = \mathbf{0}$.

The significance of risk-sensitive SDE is that it permits us to adjust the marginal distribution of noisy samples: $\tilde{p}_{t,\mathbf{r}}(\mathbf{x})$, provided with risk information \mathbf{r} . In the ideal situation, the adjusted distribution $\tilde{p}_{t,\mathbf{r}}(\mathbf{x})$ is consistent with the marginal distribution of clean samples $p_t(\mathbf{x})$. Because a nice property $\nabla_{\mathbf{x}} \ln \tilde{p}_{t,\mathbf{r}}(\mathbf{x}) = \nabla_{\mathbf{x}} \ln p_t(\mathbf{x})$ (i.e., *perturbation stability*) is satisfied in this case, the noisy sample $\tilde{\mathbf{x}}(0)$ will incur an unbiased score function to optimize the score-based model $\mathbf{s}_\theta(\mathbf{x}, t)$. In the following part, we will see that this ideal situation is achievable under some conditions and a “minimum-error” solution still exists otherwise.

1.1 Main Theory

For our theoretical study, we seek to answer the below questions:

1. In what conditions is there a *risk-sensitive SDE* to facilitate *perturbation stability*? For example, does this depend on specific noise types or the sample distribution $p_0(\mathbf{x})$?
2. If the stability property is not reachable, is there a possibility to have a solution that minimally violates the property? This is a rather subtle question. For example, we have to first define some proper measure to quantify this “violation”.
3. In the above two situations, what are the actual forms of risk-sensitive SDE? Is it generalizable to extend the current SGM (e.g., VE SDE [SSDK⁺21]) for application?

For *the first question*, our theorems provide a satisfactory answer as follows.

Theorem 1 (Simplified and Reinterpreted from Theorem 3 and Proposition 4). *The necessary and sufficient conditions for a risk-sensitive SDE to achieve perturbation stability: $\tilde{p}_{t,\mathbf{r}}(\mathbf{x}) = p_t(\mathbf{x})$, include: 1) the noisy sample $\tilde{\mathbf{x}}(0)$ is perturbed by a diagonal Gaussian noise and the risk \mathbf{r} indicates its variance; 2) the time step t is within the stability interval $\mathcal{T}(\mathbf{r})$.*

In particular, suppose the Gaussian noise is isotropic, then it suffices to represent the risk vector \mathbf{r} as a scalar r and the form of risk-sensitive SDE under this condition is as

$$\begin{cases} f(r, t) = \frac{d \ln u(t)}{dt}, \forall t \in [0, T] \\ g(r, t) = u(t)^2 \frac{d}{dt} \left(\frac{v(r, t)^2}{u(t)^2} \right), \forall t \in \mathcal{T}(r), \\ g(r, t) = 0, \forall t \in [0, T] \cap \mathcal{T}(r)^c \end{cases} \quad (2)$$

where $u(t), v(r, t)$ are continuous functions with right derivatives, satisfying

$$v(r, t)^2 = \max(v(0, t)^2 - r^2 u(t)^2, 0), \quad (3)$$

and $\mathcal{T}(r) = \{t \in [0, T] \mid v(r, t) > 0\}$ is defined as the stability interval. For zero risk $r = 0$, the above equations reduce to a ordinary risk-unaware SGM.

We can see that the ideal situation with perturbation stability is reachable *if and only if* the noise distribution is Gaussian and the time step is within the stability interval. This conclusion is also very intuitive from two perspectives: Firstly, since the backbones of *risk-sensitive SDE* and SGM are in fact a drifted Brownian motion, it is not likely that our tool can reduce the impact of a noise distribution beyond Gaussian; Secondly, noisy sample $\tilde{\mathbf{x}}(0)$ is surely less informative than the clean sample $\mathbf{x}(0)$, so it is reasonable that noisy samples cannot be used to correctly optimize the score-based model $\mathbf{s}_\theta(\mathbf{x}, t)$ at every time step t . In Theorem 3, we will also see a more general conclusion for non-isotropic Gaussian noises.

To partly answer *the third question* for Gaussian perturbation, we have the following corollary that extends VP SDE [SSDK⁺21] (i.e., the continuous relaxation of DDPM) to *risk-sensitive VP SDE*, which supports a robust optimization with isotropic Gaussian noises.

Corollary 1 (Risk-sensitive VP SDE, Simplified from Corollary 4). *Under the setting of isotropic Gaussian perturbation, the risk-sensitive SDE for VP SDE is parameterized as follows*

$$\begin{cases} f(r, t) = -\frac{1}{2}\beta(t) \\ g(r, t) = \mathbb{1}(1 > (1 + r^2)\alpha(t))\sqrt{\beta(t)} \end{cases}, \quad (4)$$

where $\mathbb{1}(\cdot)$ is an indicator function and the coefficient $\alpha(t)$ is defined as $\alpha(t) = \exp(-\int_0^t \beta(s)ds)$. The stability interval in this case is

$$\mathcal{T}(r) = \{t \in [0, T] \mid \alpha(t)^{-1} > 1 + r^2\}. \quad (5)$$

As expected, for the special case with zero risk $r = 0$, the risk-sensitive SDE reduces to an ordinary VP SDE, with $f(0, t) = -\frac{1}{2}\beta(t)$, $g(0, t) = \sqrt{\beta(t)}$, and $\mathcal{T} = [0, T]$.

Risk-sensitive VP SDE is the same as vanilla VP SDE for optimization with clean sample $(\mathbf{x}(0), r = 0)$, otherwise it will adopt a different coefficient $g(r, t)$ and a restricted set of sampling time steps $\mathcal{T}(r)$ to reduce the negative impact of noisy sample $(\tilde{\mathbf{x}}(0), r > 0)$. We will discuss this point more in Sec. 6, with detailed optimization and sampling algorithms (e.g., Algorithm 1). Corollary 4 also provides its version for non-isotropic Gaussian noises.

The second question is very important, considering the perturbation distributions in the real world might be non-Gaussian. To answer this question, we first introduce a notion called *perturbation instability* $\mathcal{S}_t(\mathbf{r})$ as follows.

Definition 2 (Perturbation Instability, Informal Version of Definition 5). *Perturbation instability $\mathcal{S}_t(\mathbf{r}) \geq 0$ is some measure that estimates the discrepancy between the marginal distribution $\tilde{p}_{t,\mathbf{r}}(\mathbf{x})$ of noisy sample $(\tilde{\mathbf{x}}(0), \mathbf{r} \neq \mathbf{0})$ and that $p_t(\mathbf{x})$ of clean sample $(\mathbf{x}(0), \mathbf{r} = \mathbf{0})$.*

The instability measure $\mathcal{S}_t(\mathbf{r})$ has two important properties: Firstly, $\mathcal{S}_t(\mathbf{r}) = 0$ if and only if the condition of perturbation stability: $\tilde{p}_{t,\mathbf{r}}(\mathbf{x}) = p_t(\mathbf{x})$, is satisfied; Secondly, the larger the measure $\mathcal{S}_t(\mathbf{r})$, the more severely the stability condition is violated.

In terms of this generalized concept of perturbation stability, we can then find the optimal parameterization of risk-sensitive SDE that minimizes the negative impact of an arbitrarily complex noise distribution on the optimization of model $\mathbf{s}_\theta(\mathbf{x}, t)$.

Theorem 2 (General Stability Theory, Simplified from Theorem 5). *Suppose the risk vector \mathbf{r} is element-wise positive and controls a family of continuous noise distributions, with each one formulated as $\rho_{\mathbf{r}}(\boldsymbol{\epsilon}) : \mathbb{R}^D \rightarrow \mathbb{R}_+$, $\int \rho_{\mathbf{r}}(\boldsymbol{\epsilon})d\boldsymbol{\epsilon} = 1$, then the optimal coefficients for the risk-sensitive SDE to minimize the instability measure $\mathcal{S}_t(\mathbf{r})$ satisfy the following equality:*

$$\begin{cases} \mathbf{v}(\mathbf{r}, t)^2 = \max(\mathbf{0}, \mathbf{v}(\mathbf{0}, t)^2 + \Psi(\mathbf{u}(t), \mathbf{r})) \\ \Psi(\mathbf{u}(t), \mathbf{r}) = 2 \left(\int \Omega(\mathbf{y})[\mathbf{y}\mathbf{y}^\top]^2 d\mathbf{y} \right)^{-1} \left(\int \Omega(\mathbf{y}) \ln |\exp(\boldsymbol{\chi}_{\mathbf{r}}(\mathbf{u}(t) \odot \mathbf{y}))| [\mathbf{y}]^2 d\mathbf{y} \right), \end{cases} \quad (6)$$

where the vectorized coefficients $\mathbf{u}(t)$, $\mathbf{v}(\mathbf{r}, t)$ come from the formal definition of risk-sensitive SDE (i.e., Definition 4) and the new terms $\Omega(\mathbf{y})$, $\boldsymbol{\chi}_{\mathbf{r}}(\cdot)$ are basic elements that defines the instability measure $\mathcal{S}_t(\mathbf{r})$ (i.e., Definition 5).

We can see that the general form of perturbation distribution $\rho_{\mathbf{r}}(\boldsymbol{\epsilon})$ incurs a very complex expression $\Psi(\mathbf{u}(t), \mathbf{r})$ in the optimal coefficient $\mathbf{v}(\mathbf{r}, t)$. In particular, if the noise $\boldsymbol{\epsilon}$ follows an isotropic Gaussian $\rho_r(\boldsymbol{\epsilon}) = \mathcal{N}(\boldsymbol{\epsilon}; \mathbf{0}, r\mathbf{I})$, then we can verify that $\Psi(u(t), r) = r^2 u(t)^2$ regardless of the weight function $\Omega(\mathbf{y})$, which is consistent with our previous conclusion: Theorem 1. Another complication of non-Gaussian noise is that: even for some isotropic noise distribution $\rho_{\mathbf{r}}(\boldsymbol{\epsilon})$, the term $\Psi(\mathbf{u}(t), \mathbf{r})$ appearing in coefficient $\mathbf{v}(\mathbf{r}, t)$ might have different expressions in different dimensions. Therefore, distinct from our Theorem 1, the vectorized coefficients $\mathbf{u}(t), \mathbf{v}(\mathbf{r}, t)$ cannot be simplified into scalar functions (e.g., $u(t), v(\mathbf{r}, t)$) for isotropic noise perturbation.

To finally answer *the third question* for non-Gaussian noises, we have the below corollary that extends VE SDE [SSDK⁺21] (a type of SGM also used in Song et al. [SDCS23]) to *risk-sensitive VE SDE*, which supports a robust optimization with Cauchy noises.

Corollary 2 (Risk-sensitive VE SDE, Simplified from Corollary 5). *For some properly defined weight function $\Omega(\mathbf{y})$ and an isotropic Cauchy perturbation specified by a scale r as*

$$\rho_r(\boldsymbol{\epsilon}) = \prod_{j=1}^D \left(\pi \left(r + \frac{\epsilon_j^2}{r} \right) \right)^{-1}, \quad \boldsymbol{\epsilon} = [\epsilon_1, \epsilon_2, \dots, \epsilon_D]^\top,$$

the minimally-unstable risk-sensitive SDE for VE SDE has coefficients as

$$\begin{cases} f(r, t) = 0 \\ g(r, t) = \mathbb{1} \left(\sigma(t)^2 > \sigma(0)^2 + \frac{D+2}{D+5} r^2 \right) \sqrt{\frac{d\sigma(t)^2}{dt}}, \end{cases} \quad (7)$$

Notably, for the setting with no risk $r = 0$, risk-sensitive VE SDE reduces to the ordinary risk-unaware VE SDE, which has fixed coefficients $f(0, t) = 0, g(0, t) = \sqrt{d\sigma(t)^2/dt}$.

With a heavy tail in the distribution, Cauchy noise has a high probability to drift a clean sample far away, exhibiting a very distinct behavior from Gaussian noises. In Appendix C, our numerical experiments (e.g., Fig. 4) show that risk-sensitive VE SDE rarely generates outliers, indicating that the optimal risk-sensitive SDE is very effective in reducing the negative impact of Cauchy-corrupted samples. Corollary 5 also provide its version for non-isotropic Cauchy noises.

1.2 Wide Applications

The problem formulation of our paper: noisy sample $\tilde{\mathbf{x}}(0)$ paired with risk vector \mathbf{r} (i.e., accessible information of data quality), is not only rarely seen in the field of generative models, but also highly motivated by real-world applications.

Data with Accessible Risks. In many cases, data are naturally born with information indicating their quality. Here are some examples from the biological and sensor domains:

- Polymerase chain reaction (PCR) is widely used In DNA sequencing to produce genomic data. Since the accuracy of PCR is largely affected by the Guanine-Cytosine content (GC-content), researchers typically regard this information as a primary indicator of the data quality [KK14, LDB17];

- Laser radars resort to laser beams to generate data, indicating the spatial positions of physical objects. This type of sensor data tends to be very noisy, so the radars also provide the engineers with other data sources, such as light strength [SC05] and device states (e.g., excessive voltage and temperature) [CP96], which reflect the data quality;
- Gyroscopes are commonly used in navigation and robotics, which measure the angular velocity of an object. This type of sensor can inherently estimate the data quality to provide engineers with more information, including bias (offset from true value) [KJCT12] and scale factor (deviation from the expected sensitivity) [TWY17].

Recently, there is a growing trend towards applying generative models to scientific (e.g., AI for Science) [CY22, HZXW23] and industrial data (e.g., Smart Manufacturing) [KVJ23, SSGL23]. Including the above examples, those types of data are generally noisy and come with risk information, where our proposed *risk-sensitive SDE* will play a key role.

Data without Available Risks. There are also situations where the risk information \mathbf{r} for noisy sample $\tilde{\mathbf{x}}(0)$ is not available. However, since our definition of the risk vector \mathbf{r} is not limited, it is very likely that one can find an alternative to the vector in a low-effort manner, without resorting to manual annotation and expert knowledge. Typical examples are time series and tabular data in the medical domain (e.g., MIMIC dataset [JPS⁺16]). Specifically, because these two types of medical data either are irregular [SHSL20] or have missing values [LT20], one will preprocess the data with interpolation and imputation before using them. Such preprocessing techniques are commonly not fully accurate, leading the final data to be noisy. In this situation, there are at least two very efficient ways to harvest the risk information:

- Some interpolation and imputation models can inherently quantify the uncertainties of their predictions. For example, Gaussian Process [M⁺98] and MissForest [SB12]. The uncertainties provided by these models can be treated as the risk information;
- There are a number of approaches (e.g., Bayesian Dropout [GG16]) in the field of Bayesian Deep Learning [KG17], which estimate the prediction uncertainty of a black-box model. If a preprocessing tool provides no extra information for its output, one can apply such a method to construct the risk vector.

Even for high-quality image data, the concept of risk information still applies and it is convenient to find the risk vector. For example, images in the ImageNet dataset [DDS⁺09] are of various sizes. To train a deep learning model (e.g., GAN [GPAM⁺20]) on that dataset, one has to first let all images have the same shape. In this way, a clear image of a small shape $H \times W$ will be expanded to a fuzzy image of a big shape $H' \times W'$. This type of sample is certainly noisy for the model and one can regard this ratio $\sqrt{(H'W')/(HW)} - 1$ as the risk information.

Determination of the Noise Types. A question might arise: How can we determine the noise type for applying the risk-sensitive SDE? In some cases, we can infer it based on the mechanism that generates risk vectors. For example, the arrival time of an unobserved sample in a continuous-time Markov Chain [And12] has an exponential distribution. In other scenarios where the risk-generating mechanism is unknown, we can suppose the noise is Gaussian, similar to the treatments in Conformal Prediction [ZDJR23, AB21] and Kalman Filter [KB⁺18]. In Appendix C, our numerical experiments (e.g., Table 1) show that this assumption works quite well.

2 Related Work

To our knowledge, the problem formulation of our paper: noisy sample $\tilde{\mathbf{x}}(0)$ associated with *risk information* \mathbf{r} , has not been considered in previous generative models and our proposed *risk-sensitive SDE* is also the first method to solve this problem. In the following, we provide an overview of relevant papers, grouped in terms of methodology and the setting.

Methodology Related. An alternative way to address our introduced problem is to adopt *conditional diffusion models* [DN21, HS21], though there is no such work in the literature. This type of conditional models can utilize extra information to generate samples with desired properties. For our problem, one can treat the risk vector as that “extra information” and apply these techniques to let SGM generate low-risk samples. We name this way as *risk-conditional SGM* in this paper and provide three different implementations in Appendix A.

The main problem with risk-conditional SGM is that it might lead to a biased sampling distribution. To understand this point, note that conditional models essentially learn a joint distribution of samples and risk vectors. If one applies risk-conditional generation, which means a preference is imposed towards less noisy samples during generation, then the regions that are correlated with a high noise level in the sampling space tend to be ignored, yielding an unbalanced distribution of generated samples. In contrast to this baseline, our risk-sensitive diffusion models directly learn the underlying true distribution of noisy samples, with no preference bias for sampling. In Appendix C, some numerical experiments (e.g., Fig. 3) confirm our above claims.

Setting Related. Some previous works [OXLC23, KNJ⁺24] in the field of generative models also considered the problem of imperfect data. However, their settings are mostly a particular case of ours and can not be applied more broadly as our method. Below are two examples:

- Ambient Diffusion [DSD⁺24] addresses the setting of images with missing pixels. As discussed in Sec. 1.2, missingness is a typical use case of our method: risk-sensitive SDE, which can be applied to a more general case: “noisy pixels”;
- Unbiased Diffusion Model [KNJ⁺24] considers the presence of both a biased dataset and a clean dataset and, thus, tackled a particular case of our method. If one assigns risk 1 to the samples of biased dataset and risk 0 to those of the clean dataset, then our method can also learn an unbiased diffusion model. However, our method supports a much more broad range of settings. In particular, this work does not consider the situation where different noisy samples might have different risks, which is very common for application;

There are also some works about noisy data but have a totally different setting from ours. For example, Na et al. [NKB⁺24] consider noisy labels instead of noisy samples.

3 Preliminaries

3.1 Background of SGM

While score-based generative models (SGM or diffusion models) have different versions and variants, we adopt the formulation of Song et al. [SSDK⁺21], which generalizes DDPM [HJA20], SMLD [SE19], VDM [DN21], etc.

At the core of SGM lies a *diffusion process*, which drives data samples $\mathbf{x}(0) \sim p_0(\mathbf{x}(0))$ (i.e., a finite-dimensional vector) towards noise $\mathbf{x}(T) \sim p_T(\mathbf{x}(T))$ at time $T \in \mathbb{R}^+$, and can be expressed through a stochastic differential equation (SDE) [Itô44]:

$$d\mathbf{x}(t) = f(t)\mathbf{x}(t)dt + g(t)d\mathbf{w}(t), \quad (8)$$

where $\mathbf{w}(t)$ is a standard Wiener process, $f(t)\mathbf{x}(t) : \mathbb{R} \times \mathbb{R}^d \rightarrow \mathbb{R}^d$ is a predefined vector-valued function that specifies the drift coefficient, and $g(t) : \mathbb{R} \rightarrow \mathbb{R}$ is a predetermined scalar-valued function that specifies the diffusion coefficient. We call p_T the prior distribution, which is fixed and retains no information of p_0 via a proper design of coefficients $\mathbf{f}(t), g(t)$.

Interestingly, the *reverse process* (i.e., reverse version of the diffusion process) also follows an SDE. For a process of the form as Eq. (8), it shapes as:

$$d\mathbf{x}(t) = (f(t)\mathbf{x}(t) - g(t)^2 \nabla_{\mathbf{x}(t)} \ln p_t(\mathbf{x}(t)))dt + g(t)d\bar{\mathbf{w}}(t) \quad (9)$$

which runs another standard Wiener process $\bar{\mathbf{w}}(t)$ backward in time. For generative purposes, we can sample randomly from the prior distribution p_T and use the reverse process to map such samples into data samples that will follow p_0 , that is, the distribution of inputs. The challenge is to determine the expression $\nabla_{\mathbf{x}} \ln p_t(\mathbf{x})$ in the backward process (known as the score function) since the term is analytically intractable in most cases. A common practice [SE19] is to use an approximation called the score-based model $\mathbf{s}_\theta(\mathbf{x}, t)$, for instance, a neural network.

To optimize the score model towards the score function, previous works [SE19, SSDK⁺21] derived the following score-matching loss:

$$\mathcal{L} = \mathbb{E}_{(t, \mathbf{x}_0, \mathbf{x}_t)} [\lambda(t) \|\mathbf{s}_\theta(\mathbf{x}(t), t) - \nabla_{\mathbf{x}(t)} \ln p_t(\mathbf{x}(t))\|_2^2], \quad (10)$$

where the weight $\lambda(t) : [0, T] \rightarrow \mathbb{R}^+$ is generally set uniformly. Importantly, it is common [SSDK⁺21] to adopt an upper bound of the above loss to fit the model $\mathbf{s}_\theta(\mathbf{x}(t), t)$ with the kernel $p_{t|0}(\mathbf{x}(t) | \mathbf{x}(0))$ (i.e., the density of $\mathbf{x}(t)$ conditioning on $\mathbf{x}(0)$).

3.2 Problem Formulation

For standard SGM, the observed sample $\mathbf{x}(0) \in \mathbb{R}^D$ is assumed to be without *noise perturbation*. However, this simplification does not apply to many real-world situations. Fig. 1 shows an example of medical time series, which consists of irregularly spaced observations. To apply SGM to such data, one has to first fill in the missing values with some interpolation method [RCD19], resulting in noises in the form of interpolation errors.

Misguidance effect of Noisy Samples. Noisy sample $\tilde{\mathbf{x}}(0)$ intuitively has a negative impact on the optimization of score-based model $\mathbf{s}_\theta(\mathbf{x}, t)$. For this point, a solid explanation is as below.

Remark 1. *In the standard case with only clean sample $\mathbf{x}(0)$, the score-based model $\mathbf{s}_\theta(\mathbf{x}, t)$ is optimized to match the score function $\nabla_{\mathbf{x}} \ln p_t(\mathbf{x})$. Since noisy sample $\tilde{\mathbf{x}}(0)$ has a different initial distribution $\tilde{p}_0(\mathbf{x})$ from that $p_0(\mathbf{x})$ of clean sample $\mathbf{x}(0)$, their marginal distributions $\tilde{p}_t(\mathbf{x}), p_t(\mathbf{x})$ at time step t will also be different, with the same diffusion process (i.e., Eq. (8)). As a result, we have $\nabla_{\mathbf{x}} \ln \tilde{p}_t(\mathbf{x}) \neq \nabla_{\mathbf{x}} \ln p_t(\mathbf{x})$, indicating that noisy sample $\tilde{\mathbf{x}}(0)$ causes a wrong objective $\nabla_{\mathbf{x}} \ln \tilde{p}_t(\mathbf{x})$ for optimizing the model $\mathbf{s}_\theta(\mathbf{x}(t), t)$.*

In short, we can say that noisy sample $\tilde{\mathbf{x}}(0)$ misleads the optimization of SGM.

Introduction of risk information. Although noisy samples are inescapable in some situations, they are usually with additional information, estimating the potential risk of using them. Following the previous example, a Gaussian process [M⁺98] that interpolates the missing samples in Fig. 1 naturally provides uncertainty information (i.e., confidence intervals) for each prediction. We can thus pair every possibly noisy sample $\tilde{\mathbf{x}}(0) = [\tilde{x}_1(0), \tilde{x}_2(0), \dots, \tilde{x}_D(0)]^\top$ with its risk information \mathbf{r} , available for free. While risk \mathbf{r} is defined in a very general way in Definition 3, its concrete form depends on the noise type. For example, in the case of *non-isotropic Gaussian perturbation*, the risk \mathbf{r} is a vector $\mathbf{r} = [r_1(0), r_2(0), \dots, r_D(0)]^\top$ of the same D dimensions as the sample $\tilde{\mathbf{x}}(0)$, indicating its entry-wise data quality. The closer to 0 the value in each entry $r_i \in \mathbb{R}^+ \cup \{0\}$ of \mathbf{r} is, the higher the expected quality, where $r_i = 0$ indicates that entry $\tilde{x}_i(0)$ is clean.

Provided with the risk vector \mathbf{r} , an ideal generative model could draw information from both risky ($\tilde{\mathbf{x}}(0), \mathbf{r} \neq \mathbf{0}$) and clean samples ($\tilde{\mathbf{x}}(0) = \mathbf{x}(0), \mathbf{r} = \mathbf{0}$), but this model was only optimized towards the distribution of clean samples: $p_0(\mathbf{x})$.

3.3 Basic Definitions

The risk information \mathbf{r} in our problem formulation is defined as follows.

Definition 3 (Risk Vector). *The risk information \mathbf{r} shapes as a vector that is element-wise non-negative and controls a family of continuous noise distributions:*

$$\mathcal{P}_\epsilon = \left\{ \rho_{\mathbf{r}}(\epsilon) : \mathbb{R}^D \rightarrow \mathbb{R}_+, \int \rho_{\mathbf{r}}(\epsilon) d\epsilon = 1 \mid \mathbf{r} \neq \mathbf{0} \right\}, \quad (11)$$

with each one perturbing clean sample $\mathbf{x}(0) \sim p_0(\mathbf{x}(0))$ into noisy sample $\tilde{\mathbf{x}}(0) = \mathbf{x}(0) + \epsilon$, which is with respect to a distribution as

$$\tilde{p}_{0,\mathbf{r}}(\tilde{\mathbf{x}}(0)) = \int p_0(\mathbf{x}(0)) \rho_{\mathbf{r}}(\tilde{\mathbf{x}}(0) - \mathbf{x}(0)) d\mathbf{x}(0). \quad (12)$$

For zero risk $\mathbf{r} = \mathbf{0}$, it means the sample $\tilde{\mathbf{x}}(0) \equiv \mathbf{x}(0)$ is noise-free.

Remark 2. *This definition might not seem intuitive. For better understanding, let us take isotropic Gaussian perturbation as an example. In that case, the risk vector \mathbf{r} can be simplified as a scalar r and the family of noise distributions \mathcal{P}_r is as $\{\mathcal{N}(\mathbf{0}, r\mathbf{I}) \mid r > 0\}$.*

In light of the *misguidance effect* of noisy sample $\tilde{\mathbf{x}}(0)$, we aim to seek an alternative diffusion process parameterized by the risk \mathbf{r} , such that noisy sample ($\tilde{\mathbf{x}}(0), \mathbf{r}$) under this process has the same

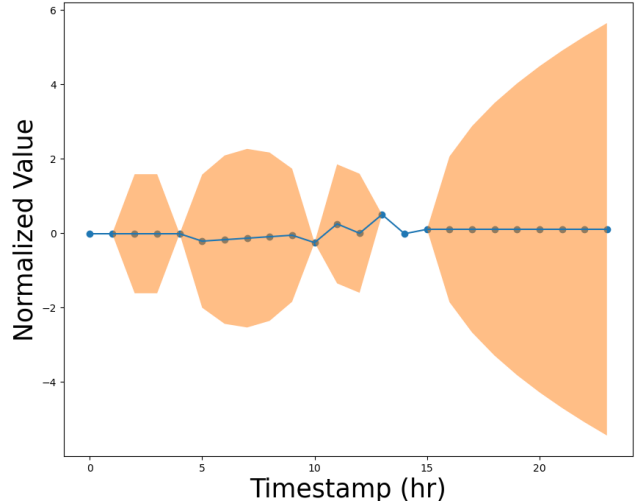


Figure 1: A segment of irregular time series from MIMIC [JPS⁺16]. The data points outside the orange region (i.e., 95% confidence intervals) are observed, and a Gaussian process interpolates the ones within the area.

distribution $\tilde{p}_{t,\mathbf{r}}(\mathbf{x})$ at some iteration t in $[0, T]$ as that of clean sample $\mathbf{x}(0)$ under the ordinary diffusion process: $p_t(\mathbf{x})$. For iteration t where the equality $\tilde{p}_{t,\mathbf{r}}(\mathbf{x}) = p_t(\mathbf{x})$ holds, the score function of noisy samples: $\nabla_{\mathbf{x}} \ln \tilde{p}_{t,\mathbf{r}}(\mathbf{x})$, can be used to safely optimize model $\mathbf{s}_{\theta}(\mathbf{x}, t)$. The new process chosen in this spirit is a specific choice of SDE whose parameterization includes the risk \mathbf{r} . We name such an SDE as *risk-sensitive SDE*. Its strict definition is as follows.

Definition 4 (Risk-sensitive SDE). *For a noisy sample $\tilde{\mathbf{x}}(0)$ with risk vector \mathbf{r} , the risk-sensitive SDE is a type of SDE that incorporates the risk \mathbf{r} into its coefficients, extending a sample vector $\tilde{\mathbf{x}}(0)$ into a dynamics $\{\tilde{\mathbf{x}}(t)\}_{t \in [0, T]}$ as*

$$d\tilde{\mathbf{x}}(t) = (\mathbf{f}(\mathbf{r}, t) \odot \tilde{\mathbf{x}}(t))dt + \mathbf{g}(\mathbf{r}, t) \odot d\mathbf{w}(t), \quad (13)$$

where \odot stands for the Hadamard product, and the coefficient functions $\mathbf{f}(\mathbf{r}, t), \mathbf{g}(\mathbf{r}, t)$ are everywhere continuous with right derivatives.

Remark 3. *For $\mathbf{r} = \mathbf{0}$, the above SDE is fed with clean sample $\mathbf{x}(0)$ and corresponds to a standard SGM (e.g., VE-SDE [SSDK⁺ 21]) with risk-unaware coefficients $\mathbf{f}(\mathbf{0}, t), \mathbf{g}(\mathbf{0}, t)$. We refer to this particular case as risk-unaware SDE. We intentionally define risk-sensitive SDEs to generalize common diffusion models; for example, choosing $\mathbf{f}(\mathbf{0}, t) = -(1/2)\beta(t)\mathbf{1}, \mathbf{g}(\mathbf{0}, t) = \sqrt{\beta(t)}\mathbf{1}, \beta(t) : [0, T] \rightarrow \mathbb{R}^+$, we recover the SDE for both VP-SDE [SSDK⁺ 21] and DDPM [HJA20].*

Remark 4. *One might notice that risk-sensitive SDE is in fact more expressive than the ordinarily defined diffusion process (i.e., Eq. (8)): The risk-sensitive coefficients $\mathbf{f}(\mathbf{r}, t), \mathbf{g}(\mathbf{r}, t)$ are vectors (i.e. non-isotropic), while risk-unaware coefficients $f(t), g(t)$ are just scalars (i.e., isotropic). In Theorem 3, we will see this setting is essential for non-isotropic perturbation.*

Remark 5. *Similar to risk-unaware SDE, risk-sensitive SDE also has a backward version in time: reverse process. Because this notion is not used in proving our theorems, we provide its concrete expression and the derivation details in Appendix B.*

As previously discussed, we aim to find a type of risk-sensitive SDE that satisfies a nice property at some time step t : $\tilde{p}_{t,\mathbf{r}}(\mathbf{x}) = p_t(\mathbf{x})$, which we defined as *perturbation stability*. While this condition is indeed possible to reach for Gaussian noises, we will see in Theorem 5 that it is not achievable in the case of non-Gaussian perturbation. Therefore, we have to introduce a new ‘‘criterion’’ that extends the concept of *perturbation stability*, measuring how much the stability is violated. With this type of criterion, we can score all the coefficient candidates of a risk-sensitive SDE and search for the best candidate, which minimizes the stability violation.

Because probability densities are uniquely determined by their *cumulant-generating functions* (i.e., log-characteristics functions) [Chu01], an obvious way to define the criterion is to measure the mean square error [Wei05] between the cumulant-generating function of $\tilde{p}_{t,\mathbf{r}}(\mathbf{x})$ and that of $p_t(\mathbf{x})$. A formal definition is in the following.

Definition 5 (Measure of Perturbation Instability). *For a given risk vector \mathbf{r} and time step t , the perturbation instability $\mathcal{S}_t(\mathbf{r})$ of a risk-sensitive SDE (as defined in Eq. (13)) measures the discrepancy between its marginal density $\tilde{p}_{t,\mathbf{r}}(\mathbf{x})$ for a noisy sample $\tilde{\mathbf{x}}(0)$ and that of the ordinary diffusion process $p_t(\mathbf{x})$ for a clean sample $\mathbf{x}(0)$ as:*

$$\mathcal{S}_t(\mathbf{r}) = \sup_{p_0(\mathbf{x})} \left(\int_{\mathbb{R}^D} \Omega(\mathbf{y}) \left| \tilde{\chi}_{t,\mathbf{r}}(\mathbf{y}) - \chi_t(\mathbf{y}) \right|^2 d\mathbf{y} \right), \quad (14)$$

where $\Omega(\mathbf{y}) : \mathbb{R}^D \rightarrow \mathbb{R}^+$ is a positive weight function and $|\cdot|$ is the complex modulus. In particular, $\tilde{\chi}_{t,\mathbf{r}}(\mathbf{y}), \chi_t(\mathbf{y})$ respectively stand for the cumulant-generating functions [Chu01] of $\tilde{p}_{t,\mathbf{r}}(\mathbf{x}), p_t(\mathbf{x})$, which both depends on the distribution of real samples: $p_0(\mathbf{x})$.

Remark 6. The weight function $\Omega(\mathbf{y})$ can be arbitrarily selected as long as the resulting integral is finite. Following the convention in signal processing [S⁺97], an appropriate candidate is $\chi_t(\mathbf{y})$ because its value indicates the importance of \mathbf{y} in reconstructing the distribution $p_t(\mathbf{x})$ from its version $\chi_t(\mathbf{y})$ in the frequency domain.

Remark 7. Extending our terminology, we say a risk-sensitive SDE achieves perturbation stability if and only if it also satisfies $\mathcal{S}_t(\mathbf{r}) = 0$. The forward direction of this claim is obvious and the reverse will be proved later in Lemma 3. However, we will see later (Sec. 5) that such stability is not always reachable. In that case, we say that a risk-sensitive SDE that achieves the infimum of $\mathcal{S}_t(\mathbf{r})$ has the property of minimum instability.

The significance of perturbation stability is that, when this property holds, then the desired equality $\nabla_{\mathbf{x}} \ln \tilde{p}_t(\mathbf{x}) = \nabla_{\mathbf{x}} \ln p_t(\mathbf{x})$ will also hold. In this situation, the score-based model $\mathbf{s}_\theta(\mathbf{x}, t)$ can be robustly optimized with noisy samples $(\tilde{\mathbf{x}}(0), \mathbf{r} \neq \mathbf{0})$.

4 Stability for Gaussian Perturbation

In this section, we aim to find the optimal *risk-sensitive coefficients* $\mathbf{f}(\mathbf{r}, t), \mathbf{g}(\mathbf{r}, t)$ that let the *risk-sensitive SDE* achieves stability under Gaussian perturbation. We will first prove a lemma about the kernel of risk-sensitive SDE and then dive into the main theorem.

4.1 Risk-sensitive Kernel

For analysis purpose, we provide a lemma that determines the form of kernel $\tilde{p}_{t|0,\mathbf{r}}(\mathbf{x} | \tilde{\mathbf{x}}(0))$ (i.e., the density of \mathbf{x} conditioning on noisy sample $\tilde{\mathbf{x}}(0)$) for a given risk-sensitive SDE.

Lemma 1 (Kernel of Risk-sensitive SDE). *Suppose we have a risk-sensitive SDE defined as Eq. (13), then its associated kernel $\tilde{p}_{t|0,\mathbf{r}}(\tilde{\mathbf{x}}(t) | \tilde{\mathbf{x}}(0))$ shapes as*

$$\left\{ \begin{array}{l} \tilde{p}_{t|0,\mathbf{r}}(\tilde{\mathbf{x}}(t) | \tilde{\mathbf{x}}(0)) = \mathcal{N}(\tilde{\mathbf{x}}(t); \bar{\mathbf{f}}(\mathbf{r}, t) \odot \tilde{\mathbf{x}}(0), \text{diag}(\bar{\mathbf{g}}(\mathbf{r}, t)^2)) \\ \mathbf{f}(\mathbf{r}, t) = \frac{d \ln \bar{\mathbf{f}}(\mathbf{r}, t)}{dt} \\ \mathbf{g}(\mathbf{r}, t)^2 = \bar{\mathbf{f}}(\mathbf{r}, t)^2 \odot \frac{d}{dt} \left(\frac{\bar{\mathbf{g}}(\mathbf{r}, t)^2}{\bar{\mathbf{f}}(\mathbf{r}, t)^2} \right) \end{array} \right., \quad (15)$$

where $\bar{\mathbf{f}}(\mathbf{r}, 0) = \mathbf{1}, \bar{\mathbf{g}}(\mathbf{r}, 0) = \mathbf{0}$ and operation *diag* expands a vector into a diagonal matrix.

Proof. For SDE, its kernel is a Gaussian distribution and the first moment is also affine if the drift term is affine [Eva12, Oks13]. Based on these facts, we can suppose that the kernel $\tilde{p}_{t|0,\mathbf{r}}(\tilde{\mathbf{x}}(t) | \tilde{\mathbf{x}}(0))$ of risk-sensitive SDE has the following form:

$$\tilde{p}_{t|0,\mathbf{r}}(\tilde{\mathbf{x}}(t) | \tilde{\mathbf{x}}(0)) = \mathcal{N}(\tilde{\mathbf{x}}(t); \bar{\mathbf{F}}(\mathbf{r}, t)\tilde{\mathbf{x}}(0), \bar{\mathbf{G}}(\mathbf{r}, t)^2), \quad (16)$$

where $\bar{\mathbf{F}}(\mathbf{r}, t), \bar{\mathbf{G}}(\mathbf{r}, t)$ are undetermined functions that output diagonal matrices.

Considering a corner case where $t \rightarrow 0$, we can infer that $\bar{\mathbf{F}}(\mathbf{r}, 0) = \mathbf{I}$ and $\bar{\mathbf{G}}(\mathbf{r}, 0) = \mathbf{0}$. For $t > 0$, assume $\delta t > 0$ and $\delta t \approx 0$, then we have

$$\begin{aligned} \tilde{p}_{t+\delta t|0,\mathbf{r}}(\tilde{\mathbf{x}}(t+\delta t) | \tilde{\mathbf{x}}(0)) &= \int \tilde{p}_{t+\delta t|0,\mathbf{r}}(\tilde{\mathbf{x}}(t+\delta t), \tilde{\mathbf{x}}(t) | \tilde{\mathbf{x}}(0)) d\tilde{\mathbf{x}}(t) \\ &= \int \tilde{p}_{t+\delta t|t,\mathbf{r}}(\tilde{\mathbf{x}}(t+\delta t) | \tilde{\mathbf{x}}(t)) \tilde{p}_{t|0,\mathbf{r}}(\tilde{\mathbf{x}}(t) | \tilde{\mathbf{x}}(0)) d\tilde{\mathbf{x}}(t). \end{aligned} \quad (17)$$

Note that $\tilde{p}_{t+\delta t|t,\mathbf{r}}(\tilde{\mathbf{x}}(t+\delta t) | \tilde{\mathbf{x}}(t), \tilde{\mathbf{x}}(0)) = \tilde{p}_{t+\delta t|t,\mathbf{r}}(\tilde{\mathbf{x}}(t+\delta t) | \tilde{\mathbf{x}}(t))$ because of the Markov property. For notational convenience, we represent the risk-sensitive SDE as

$$d\tilde{\mathbf{x}}(t) = \mathbf{F}(\mathbf{r}, t)\tilde{\mathbf{x}}(t)dt + \mathbf{G}(\mathbf{r}, t)d\mathbf{w}(t). \quad (18)$$

where $\mathbf{F}(\mathbf{r}, t) = \text{diag}(\mathbf{f}(\mathbf{r}, t))$ and $\mathbf{G}(\mathbf{r}, t) = \text{diag}(\mathbf{g}(\mathbf{r}, t))$. According to Eqs. (16) and (18), we can have the following equation:

$$\begin{cases} \tilde{\mathbf{x}}(t+\delta t) = \bar{\mathbf{F}}(\mathbf{r}, t+\delta t)\tilde{\mathbf{x}}(0) + \bar{\mathbf{G}}(\mathbf{r}, t+\delta t)\boldsymbol{\epsilon}_1 \\ \tilde{\mathbf{x}}(t) = \bar{\mathbf{F}}(\mathbf{r}, t)\tilde{\mathbf{x}}(0) + \bar{\mathbf{G}}(\mathbf{r}, t)\boldsymbol{\epsilon}_2 \\ \tilde{\mathbf{x}}(t+\delta t) = (\mathbf{I} + \delta t\mathbf{F}(\mathbf{r}, t))\tilde{\mathbf{x}}(t) + \sqrt{\delta t}\mathbf{G}(\mathbf{r}, t)\boldsymbol{\epsilon}_3 \end{cases}, \quad (19)$$

where $\boldsymbol{\epsilon}_1, \boldsymbol{\epsilon}_2, \boldsymbol{\epsilon}_3 \sim \mathcal{N}(\mathbf{0}, \mathbf{I})$. Combining the last two equalities, we have:

$$\mathbf{x}(t+\delta t) = (\mathbf{I} + \delta t\mathbf{F}(\mathbf{r}, t))\bar{\mathbf{F}}(\mathbf{r}, t)\mathbf{x}(0) + ((\mathbf{I} + \delta t\mathbf{F}(\mathbf{r}, t))\bar{\mathbf{G}}(\mathbf{r}, t)\boldsymbol{\epsilon}_2 + \sqrt{\delta t}\mathbf{G}(\mathbf{r}, t)\boldsymbol{\epsilon}_3). \quad (20)$$

Comparing the above two equations, we have:

$$\begin{cases} \bar{\mathbf{F}}(\mathbf{r}, t+\delta t) = (\mathbf{I} + \delta t\mathbf{F}(\mathbf{r}, t))\bar{\mathbf{F}}(\mathbf{r}, t) \\ \bar{\mathbf{G}}(\mathbf{r}, t+\delta t)^2 = (\mathbf{I} + \delta t\mathbf{F}(\mathbf{r}, t))^2\bar{\mathbf{G}}(\mathbf{r}, t)^2 + \delta t\mathbf{G}(\mathbf{r}, t)^2 \end{cases}. \quad (21)$$

Let $\delta t \rightarrow 0$, this equation can be converted into a differential form:

$$\mathbf{F}(\mathbf{r}, t) = \frac{d \ln \bar{\mathbf{F}}(\mathbf{r}, t)}{dt}, \quad \mathbf{G}(\mathbf{r}, t)^2 = \frac{d \bar{\mathbf{G}}(\mathbf{r}, t)^2}{dt} - 2 \frac{d \ln \bar{\mathbf{F}}(\mathbf{r}, t)}{dt} \bar{\mathbf{G}}(\mathbf{r}, t)^2. \quad (22)$$

If $\bar{\mathbf{G}}(\mathbf{r}, t)$ is only continuous but not differentiable, then the term $d \ln \bar{\mathbf{F}}(\mathbf{r}, t)/dt$ indicates its right derivative. Now, by converting all matrix-valued functions $\bar{\mathbf{F}}(\mathbf{r}, t)$, $\bar{\mathbf{G}}(\mathbf{r}, t)$, $\mathbf{F}(\mathbf{r}, t)$, $\mathbf{G}(\mathbf{r}, t)$ into their vector forms $\bar{\mathbf{f}}(\mathbf{r}, t)$, $\bar{\mathbf{g}}(\mathbf{r}, t)$, $\mathbf{f}(\mathbf{r}, t)$, $\mathbf{g}(\mathbf{r}, t)$, we have

$$\mathbf{f}(\mathbf{r}, t) = \frac{d \ln \bar{\mathbf{f}}(\mathbf{r}, t)}{dt}, \quad \mathbf{g}(\mathbf{r}, t)^2 = \bar{\mathbf{f}}(\mathbf{r}, t)^2 \odot \frac{d}{dt} \left(\frac{\bar{\mathbf{g}}(\mathbf{r}, t)^2}{\bar{\mathbf{f}}(\mathbf{r}, t)^2} \right), \quad (23)$$

where operations \odot and \oslash respectively denote element-wise product and division. The initial conditions for $\bar{\mathbf{F}}(\mathbf{r}, t)$, $\bar{\mathbf{G}}(\mathbf{r}, t)$ can also be directly transferred to $\bar{\mathbf{f}}(\mathbf{r}, t)$, $\bar{\mathbf{g}}(\mathbf{r}, t)$. \square

The above lemma is very useful. We will also see it in Sec. 6.

4.2 Solution for Gaussian Perturbation

Provided with Lemma 1, the following theorem gives a sufficient condition for letting the risk-sensitive SDE achieve *perturbation stability* for Gaussian noises. In Sec. 5, we will also see that this condition is both sufficient and necessary.

Theorem 3 (Risk-sensitive SDE for Gaussian Perturbation). *Suppose that we have a Gaussian family of perturbation distributions: $\mathcal{P}_\epsilon = \{\mathcal{N}(\mathbf{0}, \text{diag}(\mathbf{r}^2)) \mid \mathbf{r} \neq \mathbf{0}\}$, then the risk-sensitive SDE (as defined in Eq. (13)) parameterized as below:*

$$\begin{cases} \mathbf{f}(\mathbf{r}, t) = \frac{d \ln \mathbf{u}(t)}{dt}, \forall t \in [0, T] \\ \mathbf{g}(\mathbf{r}, t) = \mathbf{u}(t)^2 \odot \frac{d}{dt} \left(\frac{\mathbf{v}(\mathbf{r}, t)^2}{\mathbf{u}(t)^2} \right), \forall t \in \mathcal{T}(\mathbf{r}), \\ \mathbf{g}(\mathbf{r}, t) = \mathbf{0}, \forall t \in [0, T] \cap \mathcal{T}(\mathbf{r})^c \end{cases} \quad (24)$$

has the property of perturbation stability (i.e., $\mathcal{S}_t(\mathbf{r}) = 0$) for any t in

$$\mathcal{T}(\mathbf{r}) \equiv \{t \in [0, T] \mid \mathbf{v}(\mathbf{r}, t)^2 + \mathbf{r}^2 \odot \mathbf{u}(t)^2 = \mathbf{v}(\mathbf{r}, 0)^2\}, \quad (25)$$

regardless of the weight function $\Omega(\mathbf{y})$. Here $\mathcal{T}(\mathbf{r})^c$ represents the complement $\mathcal{T}(\mathbf{r})$ and $\mathbf{u}(t), \mathbf{v}(\mathbf{r}, t)$ are arbitrary functions that are everywhere continuous with right derivatives.

In particular, for zero risk $\mathbf{r} = \mathbf{0}$, the equations correspond to the associated risk-unaware diffusion process for clean sample ($\tilde{\mathbf{x}}(0) = \mathbf{x}(0), \mathbf{r} = \mathbf{0}$).

Proof. According to Lemma 1, the kernel of risk-sensitive SDE shapes as

$$\tilde{p}_{t|0, \mathbf{r}}(\tilde{\mathbf{x}}(t) \mid \tilde{\mathbf{x}}(0)) = \mathcal{N}(\tilde{\mathbf{x}}(t); \bar{\mathbf{f}}(\mathbf{r}, t) \odot \tilde{\mathbf{x}}(0), \text{diag}(\bar{\mathbf{g}}(\mathbf{r}, t)^2)), \quad (26)$$

where coefficients $\bar{\mathbf{f}}(\mathbf{r}, t), \bar{\mathbf{g}}(\mathbf{r}, t)^2$ are defined in Eq (15), \odot indicates the entry-wise product, and diag converts a vector into a diagonal matrix.

Let $\mathbf{x}(0) \in \mathbb{R}^d$ be a real sample that is without noise and we perturb it as $\tilde{\mathbf{x}}(0) = \mathbf{x}(0) + \epsilon \odot \mathbf{r}, \epsilon \sim \mathcal{N}(\mathbf{0}, \mathbf{I})$. We aim to first find the relation between risk-unaware kernel transition $p_{t|0}(\mathbf{x} \mid \mathbf{x}(0))$ and the expected risk-sensitive transition:

$$\mathbb{E}_{\tilde{\mathbf{x}}(0) \sim \mathcal{N}(\mathbf{x}(0), \text{diag}(\mathbf{r}^2))} [\tilde{p}_{t|0, \mathbf{r}}(\mathbf{x} \mid \tilde{\mathbf{x}}(0))]. \quad (27)$$

While the risk-unaware transition is simply a multivariate Gaussian:

$$\mathcal{N}(\mathbf{x}; \bar{\mathbf{f}}(\mathbf{0}, t) \odot \mathbf{x}(0), \text{diag}(\bar{\mathbf{g}}(\mathbf{0}, t)^2)), \quad (28)$$

we can expand the expected risk-sensitive transition as

$$\begin{aligned} & \int \mathcal{N}(\tilde{\mathbf{x}}(0); \mathbf{x}(0), \text{diag}(\mathbf{r}^2)) \tilde{p}_{t|0, \mathbf{r}}(\mathbf{x} \mid \tilde{\mathbf{x}}(0)) d\tilde{\mathbf{x}}(0) \\ &= \int \mathcal{N}(\tilde{\mathbf{x}}(0); \mathbf{x}(0), \text{diag}(\mathbf{r}^2)) \mathcal{N}(\mathbf{x}; \bar{\mathbf{f}}(\mathbf{r}, t) \odot \tilde{\mathbf{x}}(0), \text{diag}(\bar{\mathbf{g}}(\mathbf{r}, t)^2)) d\tilde{\mathbf{x}}(0). \end{aligned} \quad (29)$$

The second Gaussian distribution in the above equation can be reformulated as

$$\begin{aligned}
\mathcal{N}(\mathbf{x}; \cdot, \cdot) &= (2\pi)^{-D/2} |\text{diag}(\bar{\mathbf{g}}(\mathbf{r}, t)^2)|^{-1/2} \exp\left(-\frac{1}{2}(\mathbf{x} - \bar{\mathbf{f}}(\mathbf{r}, t) \odot \tilde{\mathbf{x}}(0))^\top \text{diag}(\bar{\mathbf{g}}(\mathbf{r}, t)^2)^{-1}(\cdot)\right) \\
&= \frac{(2\pi)^{-D/2}}{|\text{diag}(\bar{\mathbf{f}}(\mathbf{r}, t))|} \left| \text{diag}\left(\frac{\bar{\mathbf{g}}(\mathbf{r}, t)^2}{\bar{\mathbf{f}}(\mathbf{r}, t)^2}\right) \right|^{-1/2} \exp\left(-\frac{1}{2}\left(\tilde{\mathbf{x}}(0) - \frac{\mathbf{x}}{\bar{\mathbf{f}}(\mathbf{r}, t)}\right)^\top \text{diag}\left(\frac{\bar{\mathbf{g}}(\mathbf{r}, t)^2}{\bar{\mathbf{f}}(\mathbf{r}, t)^2}\right)^{-1}(\cdot)\right) \\
&= \frac{1}{|\text{diag}(\bar{\mathbf{f}}(\mathbf{r}, t))|} \mathcal{N}\left(\tilde{\mathbf{x}}(0), \frac{\mathbf{x}}{\bar{\mathbf{f}}(\mathbf{r}, t)}, \text{diag}\left(\frac{\bar{\mathbf{g}}(\mathbf{r}, t)^2}{\bar{\mathbf{f}}(\mathbf{r}, t)^2}\right)\right).
\end{aligned} \tag{30}$$

where $|\cdot|$ means the determinant of a matrix. According to the product rule of multivariate Gaussians [Ahr05], we can simplify the form of risk-sensitive transition as

$$\begin{aligned}
&\int \mathcal{N}(\tilde{\mathbf{x}}(0); \mathbf{x}(0), \text{diag}(\mathbf{r}^2)) \frac{1}{|\text{diag}(\bar{\mathbf{f}}(\mathbf{r}, t))|} \mathcal{N}\left(\tilde{\mathbf{x}}(0), \frac{\mathbf{x}}{\bar{\mathbf{f}}(\mathbf{r}, t)}, \text{diag}\left(\frac{\bar{\mathbf{g}}(\mathbf{r}, t)^2}{\bar{\mathbf{f}}(\mathbf{r}, t)^2}\right)\right) d\tilde{\mathbf{x}}(0) \\
&= \frac{1}{|\text{diag}(\bar{\mathbf{f}}(\mathbf{r}, t))|} \int \mathcal{N}\left(\frac{\mathbf{x}}{\bar{\mathbf{f}}(\mathbf{r}, t)}; \mathbf{x}(0), \text{diag}\left(\mathbf{r}^2 + \frac{\bar{\mathbf{g}}(\mathbf{r}, t)^2}{\bar{\mathbf{f}}(\mathbf{r}, t)^2}\right)\right) \mathcal{N}(\tilde{\mathbf{x}}(0); \cdot, \cdot) d\tilde{\mathbf{x}}(0) \\
&= \mathcal{N}\left(\mathbf{x}; \bar{\mathbf{f}}(\mathbf{r}, t) \odot \mathbf{x}(0), \text{diag}(\bar{\mathbf{f}}(\mathbf{r}, t)^2 \odot \mathbf{r}^2 + \bar{\mathbf{g}}(\mathbf{r}, t)^2)\right).
\end{aligned} \tag{31}$$

To let the two transitions equal, one must achieve the following two conditions:

$$\bar{\mathbf{f}}(\mathbf{r}, t) = \bar{\mathbf{f}}(\mathbf{0}, t), \quad \bar{\mathbf{f}}(\mathbf{r}, t)^2 \odot \mathbf{r}^2 + \bar{\mathbf{g}}(\mathbf{r}, t)^2 = \bar{\mathbf{g}}(\mathbf{0}, t)^2. \tag{32}$$

The first condition indicates that the term $\bar{\mathbf{f}}$ is independent of risk \mathbf{r} , while the second condition implies that there might exist some iteration t that the two transitions are not identical. Plus, because this term $\bar{\mathbf{g}}(\mathbf{r}, t)^2$ is always non-negative, we have

$$\bar{\mathbf{g}}(\mathbf{r}, t)^2 = \max(\bar{\mathbf{g}}(\mathbf{0}, t)^2 - \bar{\mathbf{f}}(\mathbf{0}, t)^2 \odot \mathbf{r}^2, \mathbf{0}), \tag{33}$$

which means the risk-sensitive SDE has an initial period of pure contraction, but after that, its transition kernel is equal to the real one. Note that operation \max is applied in an element-wise manner. $\bar{\mathbf{g}}(\mathbf{r}, t)^2$ might not be differentiable everywhere, but we can either locally smooth the curve or take its right derivative.

With the above derivation, we see that the following equation holds:

$$p_{t|0}(\mathbf{x} | \mathbf{x}(0)) = \mathbb{E}_{\tilde{\mathbf{x}}(0) \sim \mathcal{N}(\mathbf{x}(0), \text{diag}(\mathbf{r}^2))} [\tilde{p}_{t|0, \mathbf{r}}(\mathbf{x} | \tilde{\mathbf{x}}(0))], \tag{34}$$

if Eq. (32) holds. For the left hand, we then have

$$\mathbb{E}_{\mathbf{x}(0)} [p_{t|0}(\mathbf{x} | \mathbf{x}(0))] = \int p_0(\mathbf{x}(0)) p_{t|0}(\mathbf{x} | \mathbf{x}(0)) d\mathbf{x}(0) = p_t(\mathbf{x}). \tag{35}$$

Similarly, we apply the expectation operation $\mathbb{E}_{\mathbf{x}(0)}$ to the risk-sensitive transition:

$$\begin{aligned}
&\mathbb{E}_{\mathbf{x}(0)} \left[\mathbb{E}_{\tilde{\mathbf{x}}(0) \sim \mathcal{N}(\mathbf{x}(0), \text{diag}(\mathbf{r}^2))} [\tilde{p}_{t|0, \mathbf{r}}(\mathbf{x} | \tilde{\mathbf{x}}(0))] \right] \\
&= \int_{\mathbf{x}(0)} \int_{\tilde{\mathbf{x}}(0)} p_0(\mathbf{x}(0)) p(\tilde{\mathbf{x}}(0) | \mathbf{x}(0)) \tilde{p}_{t|0, \mathbf{r}}(\mathbf{x} | \tilde{\mathbf{x}}(0)) d\tilde{\mathbf{x}}(0) d\mathbf{x}(0) \\
&= \int_{\mathbf{x}(0)} \tilde{p}_{0, \mathbf{r}}(\tilde{\mathbf{x}}(0)) \tilde{p}_{t|0, \mathbf{r}}(\mathbf{x} | \tilde{\mathbf{x}}(0)) d\tilde{\mathbf{x}}(0) = \tilde{p}_{t, \mathbf{r}}(\mathbf{x}).
\end{aligned} \tag{36}$$

Therefore, we finally get $\tilde{p}_{t,\mathbf{r}}(\mathbf{x}) = p_t(\mathbf{x})$ (i.e., perturbation stability) for t in

$$\mathcal{T}(\mathbf{r}) \equiv \{t \in [0, T] \mid \bar{\mathbf{f}}(\mathbf{r}, t) = \bar{\mathbf{f}}(\mathbf{0}, t), \bar{\mathbf{f}}(\mathbf{r}, t)^2 \odot \mathbf{r}^2 + \bar{\mathbf{g}}(\mathbf{r}, t)^2 = \bar{\mathbf{g}}(\mathbf{0}, t)^2\}. \quad (37)$$

Now, if we replace $\bar{\mathbf{f}}(\mathbf{0}, t), \bar{\mathbf{g}}(\mathbf{r}, t)$ by $\mathbf{u}(t), \mathbf{v}(\mathbf{r}, t)$, then we get the theorem proved. \square

Remark 8. From this conclusion, we can easily see that, for a fixed coefficient $\mathbf{u}(t)$, the setup $\mathbf{v}(\mathbf{r}, t)^2 = \max(\mathbf{v}(\mathbf{r}, 0)^2 - \mathbf{r}^2 \odot \mathbf{u}(t)^2, \mathbf{0}^2)$ (where \max is an element-wise operation) maximizes the period of perturbation stability: $|\mathcal{T}(\mathbf{r})|$, leading to optimal coefficients.

Remark 9. It is apparent that stability interval $\mathcal{T}(\mathbf{r})$ shrinks as the risk \mathbf{r} increases, indicating that a noisier sample is less valuable for training. Therefore, under Gaussian perturbation, the ratio $|\mathcal{T}(\mathbf{r})|/T$ reflects how much information is contained in noisy sample $(\tilde{\mathbf{x}}(0), \mathbf{r})$.

Remark 10. If one limits the perturbation noise to be isotropically Gaussian, then the risk vector \mathbf{r} reduces to a scalar r , with $\mathcal{P}_\epsilon = \{\mathcal{N}(\mathbf{0}, r\mathbf{I}) \mid r > 0\}$. Eq. (24) and Eq. (25) in the theorem can also be simplified in terms of $\mathbf{r} = r\mathbf{1}, \mathbf{u}(t) = u(t)\mathbf{1}, \mathbf{v}(\mathbf{r}, t) = v(t)\mathbf{1}$.

In Sec. 6, we apply the above theorem to SGM (e.g., Risk-sensitive VP SDE in Corollary 4) and develop tools (e.g., simplified loss in Proposition 6) for efficient optimization. In Appendix C, our numerical experiments confirm the validity of the theorem (i.e., Fig. 2) and show that its suggested coefficients let SGM be robust to Gaussian-corrupted samples (i.e., Fig. 3).

5 Minimum Instability for General Noises

The goal of this section is to find the optimal coefficients $\mathbf{f}(\mathbf{r}, t), \mathbf{g}(\mathbf{r}, t)$ of risk-sensitive SDE for general noise perturbation. Importantly, one will see that the property of *perturbation stability*: $\mathcal{S}_t(\mathbf{r}) = 0$ is not achievable in the case of non-Gaussian perturbation. We will first prove two other conclusions and then provide the main theorem.

5.1 Spectral Representation

The first conclusion is to study the form of cumulant-generating function $\tilde{\chi}_{t,\mathbf{r}}(\boldsymbol{\omega})$.

Lemma 2 (Spectral Form of the Marginal Density). *Suppose that we have a risk-sensitive SDE as defined in Eq. (13), then the cumulant-generating function of its marginal density $\tilde{p}_{t,\mathbf{r}}(\mathbf{x})$ at time step $t \in [0, T]$: $\tilde{\chi}_{t,\mathbf{r}}(\boldsymbol{\omega})$, has a form as*

$$\tilde{\chi}_{t,\mathbf{r}}(\boldsymbol{\omega}) = \tilde{\chi}_{0,\mathbf{r}}(\bar{\mathbf{f}}(\mathbf{r}, t) \odot \boldsymbol{\omega}) - \frac{1}{2} \sum_{i=1}^D w_i^2 \bar{g}_i(\mathbf{r}, t)^2, \quad (38)$$

where terms $\bar{\mathbf{f}}(\mathbf{r}, t), \bar{\mathbf{g}}(\mathbf{r}, t)$ are defined in Eq. (15).

Proof. Based on Fokker-Planck equation [ØØ03], the marginal distribution $\tilde{p}_{t,\mathbf{r}}(\mathbf{x})$ at time step t satisfies the following partial differential equation (PDE):

$$\frac{\partial \tilde{p}_{t,\mathbf{r}}(\mathbf{x})}{\partial t} = - \sum_{i=1}^D f_i(\mathbf{r}, t) \tilde{p}_{t,\mathbf{r}}(\mathbf{x}) - \sum_{i=1}^D x_i f_i(\mathbf{r}, t) \frac{\partial \tilde{p}_{t,\mathbf{r}}(\mathbf{x})}{\partial x_i} + \frac{1}{2} \sum_{i=1}^D g_i(\mathbf{r}, t)^2 \frac{\partial^2 \tilde{p}_{t,\mathbf{r}}(\mathbf{x})}{\partial x_i^2}. \quad (39)$$

Because $\tilde{p}_{t,\mathbf{r}}(\mathbf{x})$ belongs to the function space $L^1(\mathbb{R}^D) = \{h : \mathbb{R}^D \rightarrow \mathbb{R} \mid \int |h(\mathbf{x})| d\mathbf{x} < \infty\}$, we can apply the continuous-time Fourier transform [Kra18],

$$\mathcal{F}(h(\mathbf{x}))(\boldsymbol{\omega}) = \int h(\mathbf{x}) \exp(i\boldsymbol{\omega}^\top \mathbf{x}) d\mathbf{x}, \boldsymbol{\omega} \in \mathbb{R}^D,$$

where i is the imaginary unit, to the PDE as

$$\begin{aligned} \frac{\partial \mathcal{F}(\tilde{p}_{t,\mathbf{r}}(\mathbf{x}))(\boldsymbol{\omega})}{\partial t} &= - \sum_{i=1}^D f_i(\mathbf{r}, t) \mathcal{F}(\tilde{p}_{t,\mathbf{r}}(\mathbf{x}))(\boldsymbol{\omega}) \\ &\quad - \sum_{i=1}^D f_i(\mathbf{r}, t) \mathcal{F}\left(x_i \frac{\partial \tilde{p}_{t,\mathbf{r}}(\mathbf{x})}{\partial x_i}\right)(\boldsymbol{\omega}) + \frac{1}{2} \sum_{i=1}^D g_i(\mathbf{r}, t)^2 \mathcal{F}\left(\frac{\partial^2 \tilde{p}_{t,\mathbf{r}}(\mathbf{x})}{\partial x_i^2}\right)(\boldsymbol{\omega}). \end{aligned} \quad (40)$$

According to some basic properties of the Fourier transform, we have

$$\begin{cases} \mathcal{F}\left(x_i \frac{\partial \tilde{p}_{t,\mathbf{r}}(\mathbf{x})}{\partial x_i}\right)(\boldsymbol{\omega}) = -i \frac{\partial}{\partial \omega_i} \left(\mathcal{F}\left(\frac{\partial \tilde{p}_{t,\mathbf{r}}(\mathbf{x})}{\partial x_i}\right)(\boldsymbol{\omega})\right) = -\frac{\partial}{\partial \omega_i} \left(w_i \mathcal{F}(\tilde{p}_{t,\mathbf{r}}(\mathbf{x}))(\boldsymbol{\omega})\right), \\ \mathcal{F}\left(\frac{\partial^2 \tilde{p}_{t,\mathbf{r}}(\mathbf{x})}{\partial x_i^2}\right)(\boldsymbol{\omega}) = -w_i^2 \mathcal{F}(\tilde{p}_{t,\mathbf{r}}(\mathbf{x}))(\boldsymbol{\omega}) \end{cases}, \quad (41)$$

By denoting $\mathcal{F}(\tilde{p}_{t,\mathbf{r}}(\mathbf{x}))(\boldsymbol{\omega})$ as $\boldsymbol{\varphi}_{t,\mathbf{r}}(\boldsymbol{\omega})$, we can cast Eq. (39) as

$$\frac{\partial \boldsymbol{\varphi}_{t,\mathbf{r}}(\boldsymbol{\omega})}{\partial t} = \sum_{i=1}^D w_i f_i(\mathbf{r}, t) \frac{\partial \boldsymbol{\varphi}_{t,\mathbf{r}}(\boldsymbol{\omega})}{\partial w_i} - \left(\frac{1}{2} \sum_{i=1}^D w_i^2 g_i(\mathbf{r}, t)^2\right) \boldsymbol{\varphi}_{t,\mathbf{r}}(\boldsymbol{\omega}). \quad (42)$$

In terms of the characteristic curves, we set ordinary differential equations (ODE) as

$$\frac{dt}{ds} = 1, \quad \frac{dw_i}{ds} = -w_i f_i(\mathbf{r}, t), \quad i \in [1, D] \cup \mathbb{N}, \quad \frac{d\boldsymbol{\varphi}}{ds} = \left(-\frac{1}{2} \sum_{i=1}^D w_i^2 g_i(\mathbf{r}, t)^2\right) \boldsymbol{\varphi}. \quad (43)$$

where s and \mathbb{N} are respectively a dummy variable and the set of all natural numbers. Considering the initial condition: $t(0) = 0, w_i(0) = \xi_i, \boldsymbol{\varphi}(0) = \boldsymbol{\varphi}_{0,\mathbf{r}}(\boldsymbol{\xi}), \boldsymbol{\xi} = [\xi_1, \xi_2, \dots, \xi_D]^\top$, the solutions to these ODE are formulated as

$$t(s) = s, \quad w_i(s) = \xi_i \bar{f}_i(\mathbf{r}, s)^{-1}, \quad \boldsymbol{\varphi}(s) = \boldsymbol{\varphi}_{0,\mathbf{r}}(\boldsymbol{\xi}) \exp\left(-\frac{1}{2} \sum_{i=1}^D \xi_i^2 \frac{\bar{g}_i(\mathbf{r}, s)^2}{\bar{f}_i(\mathbf{r}, s)^2}\right), \quad (44)$$

where coefficient functions $\bar{f}_i(\mathbf{r}, s), \bar{g}_i(\mathbf{r}, s)$ are of the forms as

$$\bar{f}_i(\mathbf{r}, s) = \exp\left(\int_0^s f_i(\mathbf{r}, s') ds'\right), \quad \bar{g}_i(\mathbf{r}, s) = \bar{f}_i(\mathbf{r}, s) \sqrt{\int_0^t \frac{g_i(\mathbf{r}, s')^2}{\bar{f}_i(\mathbf{r}, s')^2} ds'}. \quad (45)$$

Based on the above results, we can get the solution of $\boldsymbol{\varphi}_{t,\mathbf{r}}(\boldsymbol{\omega})$ as

$$\boldsymbol{\varphi}_{t,\mathbf{r}}(\boldsymbol{\omega}) = \boldsymbol{\varphi}_{0,\mathbf{r}}(\bar{\mathbf{f}}(\mathbf{r}, t) \odot \boldsymbol{\omega}) \exp\left(-\frac{1}{2} \sum_{i=1}^D w_i^2 \bar{g}_i(\mathbf{r}, t)^2\right), \quad (46)$$

in which $\bar{\mathbf{f}}(\mathbf{r}, t) = [\bar{f}_1(\mathbf{r}, t), \bar{f}_2(\mathbf{r}, t), \dots, \bar{f}_D(\mathbf{r}, t)]^\top$ and $\bar{\mathbf{g}}(\mathbf{r}, t) = [\bar{g}_1(\mathbf{r}, t), \bar{g}_2(\mathbf{r}, t), \dots, \bar{g}_D(\mathbf{r}, t)]^\top$. The lemma is proved by taking logarithms on both sides of the equation. \square

We can also get a similar conclusion for the term $\boldsymbol{\chi}_t(\boldsymbol{\omega})$ by setting $\mathbf{r} = \mathbf{0}$.

5.2 Necessary Condition for Achieving Stability

The second conclusion is about the necessary condition to achieve perturbation stability.

Proposition 4 (Necessary Condition for Perturbation Stability). *Given the definition (i.e., Eq. (13)) of risk-sensitive SDE, then a necessary condition for it to have the property of perturbation stability is that the perturbation results from diagonal Gaussian noises.*

Proof. Let the noise distribution be of a free form $q(\boldsymbol{\epsilon}) : \int q(\boldsymbol{\epsilon})d\boldsymbol{\epsilon} = 1; q(\boldsymbol{\epsilon}) > 0, \forall \boldsymbol{\epsilon} \in \mathbb{R}^D$, then the distribution of clean data $p_0(\mathbf{x})$ will be perturbed into a noisy one

$$\tilde{p}_{0,\mathbf{r}}(\mathbf{x}) = \int p_0(\mathbf{x}')q(\mathbf{x} - \mathbf{x}')d\mathbf{x}' = (p_0(\cdot) * q(\cdot))(\mathbf{x}), \quad (47)$$

where $*$ represents the convolution operation. Through Fourier transform, we have

$$\varphi_{0,\mathbf{r}}(\boldsymbol{\omega}) = \mathcal{F}(p_{0,\mathbf{r}}(\mathbf{x}))(\boldsymbol{\omega}) = \mathcal{F}(p_0(\mathbf{x}))(\boldsymbol{\omega}) \cdot \mathcal{F}(q(\mathbf{x}))(\boldsymbol{\omega}) = \varphi_{0,\mathbf{r}}(\boldsymbol{\omega})\phi(\boldsymbol{\omega}), \quad (48)$$

where $\phi(\boldsymbol{\omega}) := \mathcal{F}(q(\mathbf{x}))(\boldsymbol{\omega})$. Here we also suppose that $q(\boldsymbol{\epsilon}) \in L^1(\mathbb{R}^D)$.

With the above results and applying the Lemma 2, we can get the form of risk-unaware marginal distribution $p_{t,\mathbf{r}}(\mathbf{x})$ in the frequency domain as

$$\chi_t(\boldsymbol{\omega}) = \chi_0(\bar{\mathbf{f}}(\mathbf{0}, t) \odot \boldsymbol{\omega}) - \frac{1}{2} \sum_{i=1}^D w_i^2 \bar{g}_i(\mathbf{0}, t)^2, \quad (49)$$

and the one for risk-sensitive marginal distribution $\tilde{p}_{t,\mathbf{r}}(\mathbf{x})$ is as

$$\tilde{\chi}_{t,\mathbf{r}}(\boldsymbol{\omega}) = \chi_{0,\mathbf{r}}(\bar{\mathbf{f}}(\mathbf{r}, t) \odot \boldsymbol{\omega}) + \chi_q(\bar{\mathbf{f}}(\mathbf{r}, t) \odot \boldsymbol{\omega}) - \frac{1}{2} \sum_{i=1}^D w_i^2 \bar{g}_i(\mathbf{r}, t)^2, \quad (50)$$

where $\chi_q(\cdot)$ are the cumulant-generating function of noise distribution $q(\boldsymbol{\epsilon})$.

Because the Fourier transform \mathcal{F} is injective in the domain of definition $L^1(\mathbb{R}^D)$, the property $\tilde{p}_{t,\mathbf{r}}(\mathbf{x}) = p_t(\mathbf{x})$ is equivalent to the condition $\chi_t(\boldsymbol{\omega}) = \tilde{\chi}_{t,\mathbf{r}}(\boldsymbol{\omega})$. Considering function $p_0(\mathbf{x}) \in L^1(\mathbb{R}^D)$ and variable $\boldsymbol{\omega} \in \mathbb{R}^D$ are arbitrarily selected, the above two equations are equivalent indicate that the below two conditions are satisfied:

$$\bar{\mathbf{f}}(\mathbf{0}, t) = \bar{\mathbf{f}}(\mathbf{r}, t), \quad \phi(\boldsymbol{\omega}) = \exp\left(-\frac{1}{2}\boldsymbol{\omega}^\top \text{diag}\left(\frac{\bar{\mathbf{g}}(\mathbf{0}, t)^2}{\bar{\mathbf{f}}(\mathbf{0}, t)^2} - \frac{\bar{\mathbf{g}}(\mathbf{r}, t)^2}{\bar{\mathbf{f}}(\mathbf{r}, t)^2}\right)\boldsymbol{\omega}\right). \quad (51)$$

The shape of characteristic function $\phi(\boldsymbol{\omega})$ indicates that its form $q(\mathbf{x})$ in the spatial domain is a multivariate Gaussian [DD11], with the following moments:

$$\mathbb{E}_{\mathbf{x} \sim q(\mathbf{x})}[\mathbf{x}] = \mathbf{0}, \quad \text{diag}(\mathbf{r}^2) := \mathbb{E}[\mathbf{x}\mathbf{x}^\top] = \text{diag}\left(\frac{\bar{\mathbf{g}}(\mathbf{0}, t)^2}{\bar{\mathbf{f}}(\mathbf{0}, t)^2} - \frac{\bar{\mathbf{g}}(\mathbf{r}, t)^2}{\bar{\mathbf{f}}(\mathbf{r}, t)^2}\right). \quad (52)$$

Therefore, perturbation stability is only possible for Gaussian noise $\mathcal{N}(\mathbf{0}, \text{diag}(\mathbf{r}^2))$, $\mathbf{r} \in \mathbb{R}^D$. To achieve this stability, we have to pick up a risk-sensitive SDE of the form:

$$\begin{cases} d\mathbf{x}(t) = \left(\frac{d \ln \bar{\mathbf{f}}(t)}{dt} \odot \mathbf{x}(t)\right) dt + \left(\bar{\mathbf{f}}(t)^2 \odot \frac{d}{dt} \left(\frac{\bar{\mathbf{g}}(\mathbf{r}, t)^2}{\bar{\mathbf{f}}(t)^2}\right)\right) d\boldsymbol{\omega}(t), \\ \bar{\mathbf{g}}(\mathbf{r}, t)^2 = \max(\bar{\mathbf{g}}(\mathbf{0}, t)^2 - \mathbf{r}^2 \odot \bar{\mathbf{f}}(t)^2, \mathbf{0}) \end{cases}, \quad (53)$$

which is risk-unaware for iteration t in $\{t \in [1, T] \mid \bar{\mathbf{g}}(\mathbf{r}, t)^2 = \bar{\mathbf{g}}(\mathbf{0}, t)^2 - \mathbf{r}^2 \odot \bar{\mathbf{f}}(t)^2\}$. \square

Paired with Theorem 3, this proposition indicates that the necessary and sufficient conditions for a risk-sensitive SDE to achieve perturbation stability $\tilde{p}_{t,\mathbf{r}}(\mathbf{x}) = p_t(\mathbf{x})$ are: 1) noises follow diagonal Gaussian distributions; 2) the time step t is within the stability interval.

5.3 Solution for General Noises

Provided with former two conclusions, we can now prove the below main theorem.

Theorem 5 (General Theory of Perturbation Stability). *Suppose we have a family of continuous noise distributions: $\mathcal{P}_\epsilon = \{\rho_{\mathbf{r}}(\boldsymbol{\epsilon}) : \mathbb{R}^D \rightarrow \mathbb{R}^+, \int \rho_{\mathbf{r}}(\boldsymbol{\epsilon}) d\boldsymbol{\epsilon} = 1 \mid \mathbf{r} \neq \mathbf{0}\}$, controlled by a risk vector \mathbf{r} , then the optimal coefficients of the risk-sensitive SDE (as defined in Eq. (13)) that minimizes the perturbation instability $\mathcal{S}_t(\mathbf{r})$ satisfy*

$$\mathbf{v}(\mathbf{r}, t)^2 = \max(\mathbf{0}, \mathbf{v}(\mathbf{0}, t)^2 + \Psi(\mathbf{u}(t), \mathbf{r})), \quad (54)$$

in which the term $\Psi(\cdot)$ is defined as

$$\Psi(\mathbf{u}(t), \mathbf{r}) = 2 \left(\int \Omega(\mathbf{y}) [\mathbf{y}\mathbf{y}^\top]^2 d\mathbf{y} \right)^{-1} \otimes \left(\int \Omega(\mathbf{y}) \ln |\exp(\boldsymbol{\chi}_{\mathbf{r}}(\mathbf{u}(t) \odot \mathbf{y}))| [\mathbf{y}]^2 d\mathbf{y} \right) \quad (55)$$

where \otimes stands for a matrix multiplication, $\boldsymbol{\chi}_{\mathbf{r}}(\mathbf{y})$ is the cumulant-generating function of the noise distribution $\rho_{\mathbf{r}}(\boldsymbol{\epsilon})$, and $\mathbf{u}(t), \mathbf{v}(\mathbf{r}, t)$ satisfy the same conditions as in Eq. (24). Importantly, the property of perturbation stability $\mathcal{S}_t(\mathbf{r}) = \mathbf{0}$ is only possible to achieve for Gaussian perturbations of a diagonal form: $\rho_{\mathbf{r}}(\boldsymbol{\epsilon}) = \mathcal{N}(\boldsymbol{\epsilon}; \mathbf{0}, \text{diag}(\mathbf{r}^2))$.

Proof. Based on Lemma 2 and Proposition 4, we can see there is no appropriate risk-sensitive SDE to fully neutralize the negative impact of non-Gaussian noise distribution $q(\boldsymbol{\epsilon})$. Therefore, we aim to find an optimal (though not perfect) risk-sensitive SDE in this regard. Note that $p_0(\mathbf{x})$ is arbitrarily selected in space $L^1(\mathbb{R}^D)$, so condition $\bar{\mathbf{f}}(\mathbf{r}, t) = \bar{\mathbf{f}}(\mathbf{0}, t)$ still needs to hold. For $\bar{\mathbf{g}}(\mathbf{0}, t)$, we first consider the objective function to optimize:

$$\mathcal{O}_t = \int \Omega(\boldsymbol{\omega}) \left| \tilde{\boldsymbol{\chi}}_{t,\mathbf{r}}(\boldsymbol{\omega}) - \boldsymbol{\chi}_t(\boldsymbol{\omega}) \right|^2 d\boldsymbol{\omega}, \quad (56)$$

where $|\cdot|$ represents the magnitude of a complex number and $\Omega(\boldsymbol{\omega}) : \mathbb{R}^D \rightarrow \mathbb{R}^+$ is a predefined weight function. Considering Eq. (49) and Eq. (50), we have

$$\begin{aligned} \mathcal{O}_t &= \int \Omega(\boldsymbol{\omega}) \left| \frac{1}{2} \sum_{i=1}^D \omega_i^2 \bar{g}_i(\mathbf{0}, t)^2 - \frac{1}{2} \sum_{i=1}^D \omega_i^2 \bar{g}_i(\mathbf{r}, t)^2 + \boldsymbol{\chi}_{\mathbf{r}}(\bar{\mathbf{f}}(\mathbf{r}, t) \odot \boldsymbol{\omega}) \right|^2 d\boldsymbol{\omega} \\ &= \int \Omega(\boldsymbol{\omega}) \left| \frac{1}{2} \langle \boldsymbol{\omega}^2, \bar{\mathbf{g}}(\mathbf{0}, t)^2 - \bar{\mathbf{g}}(\mathbf{r}, t)^2 \rangle + \ln \left| \boldsymbol{\phi}_{\mathbf{r}}(\bar{\mathbf{f}}(\mathbf{r}, t) \odot \boldsymbol{\omega}) \right| + i \cdot \arg \left(\boldsymbol{\phi}_{\mathbf{r}}(\bar{\mathbf{f}}(\mathbf{r}, t) \odot \boldsymbol{\omega}) \right) \right|^2 d\boldsymbol{\omega} \quad (57) \\ &= \int \Omega(\boldsymbol{\omega}) \left(\frac{1}{2} \langle \boldsymbol{\omega}^2, \bar{\mathbf{g}}(\mathbf{0}, t)^2 - \bar{\mathbf{g}}(\mathbf{r}, t)^2 \rangle + \ln \left| \boldsymbol{\phi}_{\mathbf{r}}(\bar{\mathbf{f}}(\mathbf{r}, t) \odot \boldsymbol{\omega}) \right| \right)^2 d\boldsymbol{\omega} + \int \Omega(\boldsymbol{\omega}) \arg(\cdot)^2 d\boldsymbol{\omega}, \end{aligned}$$

where $\arg(\cdot)$ and $\langle \cdot, \cdot \rangle$ respectively represent the argument of a complex number and the inner product of two vectors. Plus, $\boldsymbol{\chi}_{\mathbf{r}}(\cdot)$ and $\boldsymbol{\phi}_{\mathbf{r}}(\cdot)$ are respectively the cumulant-generating and characteristic functions of noise distribution $\rho_{\mathbf{r}}(\boldsymbol{\epsilon})$.

Now, we denote $\bar{\mathbf{g}}(\mathbf{0}, t)^2 - \bar{\mathbf{g}}(\mathbf{r}, t)^2$ as a dummy variable $\mathbf{y} = [y_1, y_2, \dots, y_D]^\top$. Then, we compute the derivative of objective \mathcal{O}_t with respect to every input entry $y_j, j \in [1, D]$:

$$\frac{d\mathcal{O}_t}{dy_j} = \int \left(\Omega(\boldsymbol{\omega}) \cdot \omega_j^2 \left(\frac{1}{2} \langle \boldsymbol{\omega}^2, \mathbf{y} \rangle + \ln \left| \phi_{\mathbf{r}}(\bar{\mathbf{f}}(\mathbf{r}, t) \odot \boldsymbol{\omega}) \right| \right) \right) d\boldsymbol{\omega}. \quad (58)$$

Through setting $d\mathcal{O}_t/dy_j = 0$ for every j in $[1, D]$, we can get

$$\left\langle \left[\int \Omega(\boldsymbol{\omega}) \omega_j^2 \omega_i^2 d\boldsymbol{\omega} \right]_{i \in [1, D]}^\top, \mathbf{y} \right\rangle = -2 \int \Omega(\boldsymbol{\omega}) \omega_j^2 \ln \left| \phi_{\mathbf{r}}(\bar{\mathbf{f}}(\mathbf{r}, t) \odot \boldsymbol{\omega}) \right| d\boldsymbol{\omega}, \quad (59)$$

where $[\cdot]_{i \in [1, D]}^\top$ represents some column vector. By combining all results, we have

$$\left[\int \Omega(\boldsymbol{\omega}) \omega_i^2 \omega_j^2 d\boldsymbol{\omega} \right]_{i, j \in [1, D]} \mathbf{y} = -2 \left[\int \Omega(\boldsymbol{\omega}) \ln \left| \phi_{\mathbf{r}}(\bar{\mathbf{f}}(\mathbf{r}, t) \odot \boldsymbol{\omega}) \right| \omega_i^2 d\boldsymbol{\omega} \right]_{i \in [1, D]}^\top, \quad (60)$$

where $[\cdot]_{i, j \in [1, D]}$ represents some matrix. For notational convenience, we denote

$$\begin{cases} \left[\int \Omega(\boldsymbol{\omega}) \omega_i^2 \omega_j^2 d\boldsymbol{\omega} \right]_{i, j \in [1, D]} = \int \Omega(\boldsymbol{\omega}) [\boldsymbol{\omega} \boldsymbol{\omega}^\top]^2 d\boldsymbol{\omega} \\ \left[\int \Omega(\boldsymbol{\omega}) \ln \left| \phi_{\mathbf{r}}(\cdot) \right| \omega_i^2 d\boldsymbol{\omega} \right]_{i \in [1, D]}^\top = \int \Omega(\boldsymbol{\omega}) \ln \left| \phi_{\mathbf{r}}(\cdot) \right| [\boldsymbol{\omega}]^2 d\boldsymbol{\omega} \end{cases}. \quad (61)$$

Considering that $\mathbf{y} = \bar{\mathbf{g}}(\mathbf{0}, t)^2 - \bar{\mathbf{g}}(\mathbf{r}, t)^2$ and $\bar{\mathbf{g}}(\mathbf{r}, t)^2$ is always non-negative, we get

$$\bar{\mathbf{g}}(\mathbf{r}, t)^2 = \max \left(\bar{\mathbf{g}}(\mathbf{0}, t)^2 + 2 \left(\int \Omega(\boldsymbol{\omega}) [\boldsymbol{\omega} \boldsymbol{\omega}^\top]^2 d\boldsymbol{\omega} \right)^{-1} \left(\int \Omega(\boldsymbol{\omega}) \ln \left| \phi_{\mathbf{r}}(\bar{\mathbf{f}}(\mathbf{r}, t) \odot \boldsymbol{\omega}) \right| [\boldsymbol{\omega}]^2 d\boldsymbol{\omega} \right), \mathbf{0} \right). \quad (62)$$

For simplification, we introduce a new symbol Ψ as

$$\begin{aligned} \Psi(\mathbf{f}(\mathbf{r}, t), \mathbf{r}) &= 2 \left(\int \Omega(\boldsymbol{\omega}) [\boldsymbol{\omega} \boldsymbol{\omega}^\top]^2 d\boldsymbol{\omega} \right)^{-1} \left(\int \Omega(\boldsymbol{\omega}) \ln \left| \phi_{\mathbf{r}}(\bar{\mathbf{f}}(\mathbf{r}, t) \odot \boldsymbol{\omega}) \right| [\boldsymbol{\omega}]^2 d\boldsymbol{\omega} \right) \\ &= 2 \left(\int \Omega(\boldsymbol{\omega}) [\boldsymbol{\omega} \boldsymbol{\omega}^\top]^2 d\boldsymbol{\omega} \right)^{-1} \left(\int \Omega(\boldsymbol{\omega}) \ln \left| \exp(\chi_{\mathbf{r}}(\bar{\mathbf{f}}(\mathbf{r}, t) \odot \boldsymbol{\omega})) \right| [\boldsymbol{\omega}]^2 d\boldsymbol{\omega} \right). \end{aligned} \quad (63)$$

As a result, the optimal coefficient $\bar{\mathbf{g}}(\mathbf{r}, t)$ can be formulated as

$$\bar{\mathbf{g}}(\mathbf{r}, t)^2 = \max \left(\bar{\mathbf{g}}(\mathbf{0}, t)^2 + \Psi(\mathbf{f}(\mathbf{r}, t), \mathbf{r}), \mathbf{0} \right), \quad (64)$$

which finally proves the theorem. \square

With the above theorem, we can find the optimal risk-sensitive SDE for non-Gaussian perturbation, though its coefficient $\mathbf{g}(\mathbf{r}, t)$ might have a rather complicated form. In Sec. 6, we apply this theorem to Cauchy perturbation under the architecture of VE SDE (i.e., Corollary 5). Our numerical experiments in Appendix C also show that such a risk-sensitive VE SDE are very robust for optimization with Cauchy-corrupted samples (i.e., Fig. 4).

6 Applications to SGM

In this section, we aim to apply *risk-sensitive SDE* and our developed theorems to the practical implementations of SGM. We will show how to extend a vanilla diffusion model to its risk-sensitive versions under different noise perturbations and provide an efficient algorithm for optimizing the score-based model with risk-sensitive SDE.

6.1 Extensions under Gaussian Perturbation

In terms of Theorem 3, we have the following corollaries that extend two widely used diffusion models to their risk-sensitive versions. One of them is VE SDE [SSDK⁺21].

Corollary 3 (Risk-sensitive VE SDE for Gaussian Noises). *Under the assumption of Gaussian perturbation, the risk-sensitive SDE (as defined by Eq. (13)) for VE SDE, a commonly used risk-unaware diffusion model, is parameterized as follows:*

$$\mathbf{f}(\mathbf{r}, t) = \mathbf{0}, \quad \mathbf{g}(\mathbf{r}, t) = \mathbb{1}(\sigma(t)^2 \mathbf{1} \gtrsim \sigma(0)^2 \mathbf{1} + \mathbf{r}^2) \sqrt{\frac{d\sigma(t)^2}{dt}},$$

where $\mathbb{1}(\cdot)$ is an element-wise indicator function, \gtrsim represents the element-wise greater-than sign. The stability interval $\mathcal{T}(\mathbf{r})$ in this case is

$$\mathcal{T}(\mathbf{r}) = \left\{ t \in [0, T] \mid \sigma(t)^2 - \max_{i \in [1, D]} r_i^2 > 0 \right\}.$$

In particular, for the case of zero risk $\mathbf{r} = \mathbf{0}$, the above risk-sensitive SDE reduces to the vanilla VE SDE, with $\mathbf{f}(\mathbf{0}, t) = \mathbf{0}$, $\mathbf{g}(\mathbf{0}, t) = \sqrt{d\sigma(t)^2/dt} \mathbf{1}$, and $\mathcal{T} = [0, T]$.

Proof. For VE SDE, its risk-unaware kernel is as

$$\begin{cases} p_{t|0}(\mathbf{x}(t) \mid \mathbf{x}(0)) = \mathcal{N}(\mathbf{x}(t); \bar{\mathbf{f}}(t) \odot \mathbf{x}(0), \text{diag}(\bar{\mathbf{g}}(\mathbf{0}, t)^2)) \\ \bar{\mathbf{f}}(t) = \mathbf{1}, \quad \bar{\mathbf{g}}(\mathbf{0}, t)^2 = (\sigma(t)^2 - \sigma(0)^2) \mathbf{1} \end{cases},$$

where $\sigma(t) : [0, T] \rightarrow \mathbb{R}^+$ is an exponentially increasing function. Considering our previous conclusions (i.e., Eq. (32) and Eq. (23)) for Gaussian noises, the risk-unaware and risk-sensitive SDEs for VE SDE are parameterized as follows:

$$\begin{cases} d\mathbf{x}(t) = \mathbf{g}(\mathbf{0}, t) \odot d\mathbf{w}(t), \mathbf{g}(\mathbf{0}, t) = \mathbf{1} \sqrt{\frac{d\sigma(t)^2}{dt}} \\ d\tilde{\mathbf{x}}(t) = \mathbf{g}(\mathbf{r}, t) \odot d\mathbf{w}(t), \mathbf{g}(\mathbf{r}, t) = \mathbb{1}(\sigma(t)^2 \mathbf{1} \gtrsim \sigma(0)^2 \mathbf{1} + \mathbf{r}^2) \sqrt{\frac{d\sigma(t)^2}{dt}} \end{cases},$$

where $\mathbb{1}(\cdot)$ is an element-wise indicator function. The risk-sensitive SDE of VE SDE is of perturbation stability at iteration $t \in [0, T]$ iff the vector $\sigma(t)^2 \mathbf{1} - \mathbf{r}^2$ is positive in each entry. \square

The other is VP SDE [SSDK⁺21], the continuous version of DDPM [HJA20].

Corollary 4 (Risk-sensitive VP SDE for Gaussian Noises). *Under the assumption of Gaussian perturbation, the risk-sensitive SDE for VP SDE is parameterized as follows:*

$$\mathbf{f}(\mathbf{r}, t) = -\frac{1}{2}\beta(t)\mathbf{1}, \quad \mathbf{g}(\mathbf{r}, t) = \mathbb{1}(\mathbf{1} \gtrsim (\mathbf{1} + \mathbf{r}^2)\alpha(t)) \sqrt{\beta(t)},$$

where $\alpha(t) = \exp(-\int_0^t \beta(s) ds)$. The stability interval $\mathcal{T}(\mathbf{r})$ in this case is

$$\mathcal{T}(\mathbf{r}) = \left\{ t \in [0, T] \mid \alpha(t)^{-1} > 1 + \max_{1 \leq j \leq D} r_j^2 \right\}.$$

As expected, for the situation with zero risk $\mathbf{r} = \mathbf{0}$, the risk-sensitive SDE reduces to an ordinary VP SDE, with $\mathbf{f}(\mathbf{0}, t) = -\frac{1}{2}\beta(t)\mathbf{1}$, $\mathbf{g}(\mathbf{0}, t) = \sqrt{\beta(t)}\mathbf{1}$.

Proof. For VP SDE, its risk-unaware kernel is as

$$\begin{cases} p_{t|0}(\mathbf{x}(t) | \mathbf{x}(0)) = \mathcal{N}(\mathbf{x}(t); \bar{\mathbf{f}}(t) \odot \mathbf{x}(0), \text{diag}(\bar{\mathbf{g}}(\mathbf{0}, t)^2)) \\ \bar{\mathbf{f}}(t) = \mathbf{1} \exp\left(-\frac{1}{2} \int_0^t \beta(s) ds\right) \\ \bar{\mathbf{g}}(\mathbf{0}, t)^2 = \mathbf{1} - \mathbf{1} \exp\left(-\int_0^t \beta(s) ds\right) \end{cases},$$

where $\beta(t) : [0, T] \rightarrow \mathbb{R}^+$ is a predefined curve. Similar to our discussion about VE SDE, by using Eq. (32) and Eq. (23), the risk-unaware and risk-sensitive SDEs for VP SDE are as

$$\begin{cases} d\mathbf{x}(t) = (\mathbf{f}(t) \odot \mathbf{x}(t))dt + \mathbf{g}(\mathbf{0}, t) \odot d\mathbf{w}(t), \mathbf{f}(t) = -\frac{1}{2}\beta(t)\mathbf{1}, \mathbf{g}(\mathbf{0}, t) = \sqrt{\beta(t)}\mathbf{1} \\ d\tilde{\mathbf{x}}(t) = (\mathbf{f}(t) \odot \tilde{\mathbf{x}}(t))dt + \mathbf{g}(\mathbf{r}, t) \odot d\mathbf{w}(t), \mathbf{g}(\mathbf{r}, t) = \mathbb{1}\left(\mathbf{1} \gtrsim (\mathbf{1} + \mathbf{r}^2) \exp\left(-\int_0^t \beta(s) ds\right)\right) \sqrt{\beta(t)}. \end{cases}$$

The stability interval $\mathcal{T}(\mathbf{r})$ is as $\{t \in [0, T] \mid \exp(\int_0^t \beta(s) ds) > 1 + \max_{1 \leq j \leq D} r_j^2\}$. \square

One can apply the two corollaries to isotropic Gaussian noises by simply setting $\mathbf{r} = r\mathbf{1}$, such that coefficients $\mathbf{f}(t), \mathbf{g}(\mathbf{r}, t)$ will reduce to scalar functions. In Appendix C, our numerical experiments confirm that Risk-sensitive VP SDE can achieve stability under Gaussian perturbation (i.e., Fig. 2) and it is indeed robust to Gaussian-corrupted samples (i.e., Fig. 3).

6.2 Optimization and Sampling

In this part, we provide essential elements for applying *risk-sensitive SGM* in practice, including the loss function, optimization algorithm, and sampling algorithm. Before diving into the details, we will first prove a lemma about the stability condition.

Lemma 3 (“Not Instable” means “Stable”). *Provided with the definition of instability measure $\mathcal{S}_t(\mathbf{r})$ in Eq. (14) and suppose that distributions $p_0(\mathbf{x}), \rho_{\mathbf{r}}(\boldsymbol{\epsilon})$ are continuous. If we have $\mathcal{S}_t(\mathbf{r}) = 0$, then $\tilde{\chi}_{t,\mathbf{r}}(\mathbf{y}) = \chi_t(\mathbf{y}), \forall \mathbf{y} \in \mathbb{R}^D$ and $\tilde{p}_{t,\mathbf{r}}(\mathbf{x}) = p_t(\mathbf{x}), \forall \mathbf{x} \in \mathbb{R}^D$ both hold.*

Proof. We prove the first equality by contradiction. Suppose that $\tilde{\chi}_{t,\mathbf{r}}(\mathbf{y}) \neq \chi_t(\mathbf{y})$ for some point $\mathbf{y}' \in \mathbb{R}^D$, then there is a closed region $U \subset \mathbb{R}^D$ that satisfies $|U| > 0$ and $\tilde{\chi}_{t,\mathbf{r}}(\mathbf{y}) \neq \chi_t(\mathbf{y}), \forall \mathbf{y} \in U$ because probabilistic densities $\tilde{\chi}_{t,\mathbf{r}}(\mathbf{y}), \chi_t(\mathbf{y})$ are both continuous everywhere. Considering that the region U is a closed set, we have the below inequalities

$$\zeta_1 = \min_{\mathbf{y} \in U} |\tilde{\chi}_{t,\mathbf{r}}(\mathbf{y}) - \chi_t(\mathbf{y})| > 0, \quad \zeta_2 = \min_{\mathbf{y} \in U} \Omega(\mathbf{y}) > 0. \quad (65)$$

With these results, we further have

$$\mathcal{S}_t(\mathbf{r}) \geq \int_U \Omega(\mathbf{y}) |\tilde{\chi}_{t,\mathbf{r}}(\mathbf{y}) - \chi_t(\mathbf{y})|^2 d\mathbf{y} > \int_U \zeta_2 \zeta_1^2 = |U| \zeta_2 \zeta_1^2 > 0, \quad (66)$$

which contradict the precondition $\mathcal{S}_t(\mathbf{r}) = 0$. Hence, we have $\tilde{\chi}_{t,\mathbf{r}}(\mathbf{y}) = \chi_t(\mathbf{y}), \forall \mathbf{y} \in \mathbb{R}^D$. We can also immediately get the second equality proved since probability densities are uniquely determined by their cumulant-generating functions. \square

It is trivial that stability condition $\tilde{p}_{t,\mathbf{r}}(\mathbf{x}) = p_t(\mathbf{x})$ indicates zero instability measure $\mathcal{S}_t(\mathbf{r}) = 0$. Therefore, an implication of the above lemma is that the two conditions are in fact equivalent if the sample $p_0(\mathbf{x})$ and noise distributions $\rho_{\mathbf{r}}(\boldsymbol{\epsilon})$ are both continuous.

Risk-free loss for noisy samples. In the following proposition, we derive the loss function for risk-sensitive SDE to robustly optimize the score-based model $\mathbf{s}_\theta(\mathbf{x}, t)$ with noisy sample $(\tilde{\mathbf{x}}(0), \mathbf{r})$. We also further simplify the loss for efficient computation.

Proposition 6 (Risk-free Loss for Robust Optimization). *Suppose that the risky sample $(\tilde{\mathbf{x}}(0) = \mathbf{x}(0) + \boldsymbol{\epsilon}, \mathbf{r})$ is generated from clean sample $(\mathbf{x}(0), \mathbf{r} = \mathbf{0})$ with some perturbation noise $\boldsymbol{\epsilon} \sim \rho_{\mathbf{r}}(\boldsymbol{\epsilon})$, then the loss of standard (i.e., risk-unaware) diffusion models at time step t :*

$$\mathcal{L}_{t, \mathbf{r}=\mathbf{0}} = \mathbb{E}_{\mathbf{x} \sim p_t(\mathbf{x})} [\|\mathbf{s}_\theta(\mathbf{x}, t) - \nabla_{\mathbf{x}} \ln p_t(\mathbf{x})\|^2],$$

is equal to the below new loss for non-zero risk $\mathbf{r} \neq \mathbf{0}$:

$$\mathcal{L}_{t, \mathbf{r}} = \mathbb{E}_{\mathbf{x} \sim \tilde{p}_{t, \mathbf{r}}(\mathbf{x})} [\|\mathbf{s}_\theta(\mathbf{x}, t) - \nabla_{\mathbf{x}} \ln \tilde{p}_{t, \mathbf{r}}(\mathbf{x})\|^2], \quad (67)$$

if the noise distribution $\rho_{\mathbf{r}}(\boldsymbol{\epsilon})$ is Gaussian and the time step t is within the stability interval $\mathcal{T}(\mathbf{r})$. Importantly, the alternative loss $\mathcal{L}_{t, \mathbf{r}}$ has another form:

$$\mathcal{L}_{t, \mathbf{r}} = \mathcal{C}_t + \mathbb{E}_{\tilde{\mathbf{x}}(0), \boldsymbol{\eta}} [\|\boldsymbol{\eta} / \mathbf{v}(\mathbf{r}, t) + \mathbf{s}_\theta(\mathbf{u}(t) \odot \tilde{\mathbf{x}}(0) + \mathbf{v}(\mathbf{r}, t) \odot \boldsymbol{\eta}, t)\|^2], \quad (68)$$

where $\tilde{\mathbf{x}}(0) \sim \tilde{p}_{0, \mathbf{r}}(\mathbf{x})$, coefficients $\mathbf{u}(t), \mathbf{v}(\mathbf{r}, t)$ are as defined in Eq. (24), $\boldsymbol{\eta} \sim \mathcal{N}(\mathbf{0}, \mathbf{I})$, and \mathcal{C}_t is a constant that does not contain the parameter $\boldsymbol{\theta}$.

Proof. Based on Theorem 3 and Lemma 3, we know that the stability condition $\tilde{p}_{t, \mathbf{r}}(\mathbf{x}) = p_t(\mathbf{x})$ is achieved in this setup. Therefore, we can derive

$$\mathcal{L}_{t, \mathbf{0}} = \mathbb{E}[\|\mathbf{s}_\theta(\mathbf{x}, t) - \nabla_{\mathbf{x}} \ln p_t(\mathbf{x})\|_2^2] = \mathbb{E}[\|\mathbf{s}_\theta(\mathbf{x}, t) - \nabla_{\mathbf{x}} \ln \tilde{p}_{t, \mathbf{r}}(\mathbf{x})\|_2^2] = \mathcal{L}_{t, \mathbf{r}}. \quad (69)$$

Therefore, the first claim of this theorem is proved.

Secondly, we aim to derive another form of the loss $\mathcal{L}_{t, \mathbf{r}}$ to make it computationally feasible. To begin with, by expanding the definition of $\mathcal{L}_{t, \mathbf{r}}$, we have

$$\begin{aligned} \mathcal{L}_{t, \mathbf{r}} &= \mathbb{E}_{\tilde{\mathbf{x}}(t) \sim \tilde{p}_{t, \mathbf{r}}(\tilde{\mathbf{x}}(t))} \left[\|\mathbf{s}_\theta(\tilde{\mathbf{x}}(t), t) - \nabla_{\tilde{\mathbf{x}}(t)} \ln \tilde{p}_{t, \mathbf{r}}(\tilde{\mathbf{x}}(t))\|_2^2 \right] \\ &= \mathbb{E} \left[\|\mathbf{s}_\theta(\tilde{\mathbf{x}}(t), t)\|_2^2 + \|\nabla_{\tilde{\mathbf{x}}(t)} \ln \tilde{p}_{t, \mathbf{r}}(\tilde{\mathbf{x}}(t))\|_2^2 - 2\mathbf{s}_\theta(\tilde{\mathbf{x}}(t), t)^\top \nabla_{\tilde{\mathbf{x}}(t)} \ln \tilde{p}_{t, \mathbf{r}}(\tilde{\mathbf{x}}(t)) \right]. \end{aligned} \quad (70)$$

Considering the following transformations:

$$\begin{aligned} \nabla_{\tilde{\mathbf{x}}(t)} \ln \tilde{p}_{t, \mathbf{r}}(\tilde{\mathbf{x}}(t)) &= \frac{\nabla_{\tilde{\mathbf{x}}(t)} \tilde{p}_{t, \mathbf{r}}(\tilde{\mathbf{x}}(t))}{\tilde{p}_{t, \mathbf{r}}(\tilde{\mathbf{x}}(t))} = \frac{\nabla_{\tilde{\mathbf{x}}(t)} \int \tilde{p}_{0, t, \mathbf{r}}(\tilde{\mathbf{x}}(0), \tilde{\mathbf{x}}(t)) d\tilde{\mathbf{x}}(0)}{\tilde{p}_{t, \mathbf{r}}(\tilde{\mathbf{x}}(t))} \\ &= \frac{\nabla_{\tilde{\mathbf{x}}(t)} \int \tilde{p}_{0, \mathbf{r}}(\tilde{\mathbf{x}}(0)) \tilde{p}_{t|0, \mathbf{r}}(\tilde{\mathbf{x}}(t) | \tilde{\mathbf{x}}(0)) d\tilde{\mathbf{x}}(0)}{\tilde{p}_{t, \mathbf{r}}(\tilde{\mathbf{x}}(t))} \\ &= \frac{\int \tilde{p}_{0, t, \mathbf{r}}(\tilde{\mathbf{x}}(0), \tilde{\mathbf{x}}(t)) \nabla_{\tilde{\mathbf{x}}(t)} \ln \tilde{p}_{t|0, \mathbf{r}}(\tilde{\mathbf{x}}(t) | \tilde{\mathbf{x}}(0)) d\tilde{\mathbf{x}}(0)}{\tilde{p}_{t, \mathbf{r}}(\tilde{\mathbf{x}}(t))} \\ &= \int \tilde{p}_{0|t, \mathbf{r}}(\tilde{\mathbf{x}}(0) | \tilde{\mathbf{x}}(t)) \nabla_{\tilde{\mathbf{x}}(t)} \ln \tilde{p}_{t|0, \mathbf{r}}(\tilde{\mathbf{x}}(t) | \tilde{\mathbf{x}}(0)) d\tilde{\mathbf{x}}(0) \\ &= \mathbb{E}_{\tilde{\mathbf{x}}(0) \sim \tilde{p}_{0|t, \mathbf{r}}(\tilde{\mathbf{x}}(0) | \tilde{\mathbf{x}}(t))} [\nabla_{\tilde{\mathbf{x}}(t)} \ln \tilde{p}_{t|0, \mathbf{r}}(\tilde{\mathbf{x}}(t) | \tilde{\mathbf{x}}(0))]. \end{aligned} \quad (71)$$

Algorithm 1 Optimization Algorithm

- 1: **repeat**
 - 2: Sample $(\tilde{\mathbf{x}}(0), \mathbf{r})$ from the dataset
 - 3: Sample time step t from *stability interval* $\mathcal{T}(\mathbf{r})$
 - 4: $\tilde{\mathbf{x}}(t) = \mathbf{u}(t) \odot \tilde{\mathbf{x}}(0) + \mathbf{v}(\mathbf{r}, t) \odot \boldsymbol{\eta}$, $\boldsymbol{\eta} \sim \mathcal{N}(\mathbf{0}, \mathbf{I})$
 - 5: Update $\boldsymbol{\theta}$ with $-\nabla_{\boldsymbol{\theta}} \|\boldsymbol{\eta} / \mathbf{v}(\mathbf{r}, t) + \mathbf{s}_{\boldsymbol{\theta}}(\tilde{\mathbf{x}}(t), t)\|^2$
 - 6: **until** converged
-

Combining the above two equations, we have

$$\begin{aligned}
 \mathcal{L}_{t,\mathbf{r}} &= \mathbb{E}_{\tilde{\mathbf{x}}(t)} \left[\|\mathbf{s}_{\boldsymbol{\theta}}(\cdot)\|_2^2 + \|\nabla_{\tilde{\mathbf{x}}(t)} \ln \tilde{p}_{t,\mathbf{r}}(\tilde{\mathbf{x}}(t))\|_2^2 - 2\mathbf{s}_{\boldsymbol{\theta}}(\tilde{\mathbf{x}}(t), t)^\top \mathbb{E}_{\tilde{\mathbf{x}}(0)} [\nabla_{\tilde{\mathbf{x}}(t)} \ln \tilde{p}_{t|0,\mathbf{r}}(\tilde{\mathbf{x}}(t) | \tilde{\mathbf{x}}(0))] \right] \\
 &= \mathbb{E}_{\tilde{\mathbf{x}}(0), \tilde{\mathbf{x}}(t)} \left[\|\mathbf{s}_{\boldsymbol{\theta}}(\cdot)\|_2^2 + \|\nabla_{\tilde{\mathbf{x}}(t)} \ln \tilde{p}_{t|0,\mathbf{r}}(\cdot)\|_2^2 - 2\mathbf{s}_{\boldsymbol{\theta}}(\tilde{\mathbf{x}}(t), t)^\top \nabla_{\tilde{\mathbf{x}}(t)} \ln \tilde{p}_{t|0,\mathbf{r}}(\tilde{\mathbf{x}}(t) | \tilde{\mathbf{x}}(0)) \right] + \mathcal{C}_t \quad (72) \\
 &= \mathbb{E}_{\tilde{\mathbf{x}}(0) \sim \tilde{p}_{0,\mathbf{r}}(\tilde{\mathbf{x}}(0)), \tilde{\mathbf{x}}(t) \sim \tilde{p}_{t|0,\mathbf{r}}(\tilde{\mathbf{x}}(t) | \tilde{\mathbf{x}}(0))} \left[\|\mathbf{s}_{\boldsymbol{\theta}}(\tilde{\mathbf{x}}(t), t) - \nabla_{\tilde{\mathbf{x}}(t)} \ln \tilde{p}_{t|0,\mathbf{r}}(\tilde{\mathbf{x}}(t) | \tilde{\mathbf{x}}(0))\|_2^2 \right] + \mathcal{C}_t,
 \end{aligned}$$

where \mathcal{C}_t is a constant that does not contain parameter $\boldsymbol{\theta}$:

$$\mathcal{C}_t = \mathbb{E}_{\tilde{\mathbf{x}}(0), \tilde{\mathbf{x}}(t)} \left[\|\nabla_{\tilde{\mathbf{x}}(t)} \ln \tilde{p}_{t,\mathbf{r}}(\tilde{\mathbf{x}}(t))\|_2^2 - \|\nabla_{\tilde{\mathbf{x}}(t)} \ln \tilde{p}_{t|0,\mathbf{r}}(\tilde{\mathbf{x}}(t) | \tilde{\mathbf{x}}(0))\|_2^2 \right]. \quad (73)$$

Finally, we only have to simplify the derivative term:

$$\begin{aligned}
 \nabla_{\tilde{\mathbf{x}}(t)} \ln \tilde{p}_{t|0,\mathbf{r}}(\tilde{\mathbf{x}}(t) | \tilde{\mathbf{x}}(0)) &= \nabla_{\tilde{\mathbf{x}}(t)} \left(\ln \mathcal{N}(\tilde{\mathbf{x}}(t); \bar{\mathbf{f}}(\mathbf{r}, t) \odot \tilde{\mathbf{x}}(0), \text{diag}(\bar{\mathbf{g}}(\mathbf{r}, t)^2)) \right) \\
 &= \nabla_{\tilde{\mathbf{x}}(t)} \left(-\frac{D}{2} \ln(2\pi) - \sum_{j=1}^D \ln \bar{g}_j(\mathbf{r}, t) - \frac{1}{2} \left\langle (\tilde{\mathbf{x}}(t) - \bar{\mathbf{f}}(\mathbf{r}, t) \odot \tilde{\mathbf{x}}(0))^2, \bar{\mathbf{g}}(\mathbf{r}, t)^{-2} \right\rangle \right) \quad (74) \\
 &= \frac{\bar{\mathbf{f}}(\mathbf{r}, t) \odot \tilde{\mathbf{x}}(0) - \tilde{\mathbf{x}}(t)}{\bar{\mathbf{g}}(\mathbf{r}, t)^2}.
 \end{aligned}$$

To conclude, the risk-free loss has a simplified form as

$$\mathcal{L}_{t,\mathbf{r}} = \mathbb{E}_{\tilde{\mathbf{x}}(0) \sim \tilde{p}_{0,\mathbf{r}}(\tilde{\mathbf{x}}(0)), \tilde{\mathbf{x}}(t) \sim \tilde{p}_{t|0,\mathbf{r}}(\tilde{\mathbf{x}}(t) | \tilde{\mathbf{x}}(0))} \left[\left\| \mathbf{s}_{\boldsymbol{\theta}}(\tilde{\mathbf{x}}(t), t) - \frac{\bar{\mathbf{f}}(\mathbf{r}, t) \odot \tilde{\mathbf{x}}(0) - \tilde{\mathbf{x}}(t)}{\bar{\mathbf{g}}(\mathbf{r}, t)^2} \right\|_2^2 \right] + \mathcal{C}_t. \quad (75)$$

Similar to DDPM [HJA20], we can further simplify this equation by Gaussian reparameterization. With the reparameterization $\tilde{\mathbf{x}}(t) = \bar{\mathbf{f}}(\mathbf{r}, t) \odot \tilde{\mathbf{x}}(0) + \bar{\mathbf{g}}(\mathbf{r}, t) \odot \boldsymbol{\epsilon}$, $\boldsymbol{\epsilon} \sim \mathcal{N}(\mathbf{0}, \mathbf{I})$, we get

$$\mathcal{L}_{t,\mathbf{r}} = \mathbb{E}_{\tilde{\mathbf{x}}(0) \sim \tilde{p}_{0,\mathbf{r}}(\tilde{\mathbf{x}}(0)), \boldsymbol{\epsilon} \sim \mathcal{N}(\mathbf{0}, \mathbf{I})} \left[\left\| \mathbf{s}_{\boldsymbol{\theta}} \left(\bar{\mathbf{f}}(\mathbf{r}, t) \odot \tilde{\mathbf{x}}(0) + \bar{\mathbf{g}}(\mathbf{r}, t) \odot \boldsymbol{\epsilon}, t \right) + \frac{\boldsymbol{\epsilon}}{\bar{\mathbf{g}}(\mathbf{r}, t)} \right\|_2^2 \right] + \mathcal{C}_t, \quad (76)$$

where time step t belongs to stability period \mathcal{T} . □

The expression of risk-free loss in Eq. (68) permits efficient computation in practice. Importantly but as anticipated, for the case of zero risk $\mathbf{r} = 0$, the term reduces to the loss function of ordinary risk-unaware diffusion models: $\mathcal{L}_{t,\mathbf{0}}$, for clean sample $\mathbf{x}(0)$.

Algorithm 2 Sampling Algorithm

- 1: Set time points $\{t_M = T, t_{M-1}, \dots, t_2, t_1 = 0\}$
 - 2: Set zero risk $\mathbf{r} = \mathbf{0}$
 - 3: $\mathbf{x}(t_M) \sim p_T(\mathbf{x}) \approx \mathcal{N}(\mathbf{x}; \mathbf{0}, \mathbf{I})$
 - 4: **for** $i = M, M - 1, \dots, 2$ **do**
 - 5: $\hat{\mathbf{b}}(\mathbf{x}(t_i), t_i) = \mathbf{f}(\mathbf{r}, t_i) \odot \mathbf{x}(t_i) - \mathbf{g}(\mathbf{r}, t_i)^2 \odot \mathbf{s}_\theta(\mathbf{x}(t_i), t_i)$
 - 6: $\boldsymbol{\eta} \sim \mathcal{N}(\mathbf{0}, (t_i - t_{i-1})\mathbf{I})$
 - 7: $\mathbf{x}(t_{i-1}) = \mathbf{x}(t_i) - \hat{\mathbf{b}}(\mathbf{x}(t_i), t_i)(t_i - t_{i-1}) - \mathbf{g}(\mathbf{r}, t_i) \odot \boldsymbol{\eta}$
 - 8: **end for**
 - 9: **return** $\mathbf{x}(0)$
-

Optimization and sampling. We respectively show the optimization and sampling procedures in Algorithm 1 and Algorithm 2. We also highlight in blue the terms that differ from vanilla diffusion models. For the optimization algorithm, when the risk is $\mathbf{0}$, the algorithm reduces to the optimization procedure of a vanilla diffusion model, with a trivial stability interval of $\mathcal{T}(\mathbf{r}) = [0, T]$. When the risk is non-zero, the risk-sensitive coefficient $\mathbf{v}(\mathbf{r}, t)$ and interval $\mathcal{T}(\mathbf{r})$ will guarantee that $\nabla_{\mathbf{x}} \ln p_t(\mathbf{x}) = \nabla_{\mathbf{x}} \ln \tilde{p}_{t, \mathbf{r}}(\mathbf{x})$ for $t \in \mathcal{T}(\mathbf{r})$, such that the noisy sample $(\tilde{\mathbf{x}}(0), \mathbf{r} \neq \mathbf{0})$ can be used to safely optimize the score-based model $\mathbf{s}_\theta(\mathbf{x}, t)$.

For the sampling algorithm, by setting zero risk $\mathbf{r} = \mathbf{0}$, the coefficients $\mathbf{f}(\mathbf{r}, t), \mathbf{g}(\mathbf{r}, t)$ become compatible with the model $\mathbf{s}_\theta(\mathbf{x}, t)$ and together generate high-quality sample $\mathbf{x}(0)$. Our model will generate only clean samples $(\mathbf{x}(0), \mathbf{r} = \mathbf{0})$, but it was already able to capture the rich distribution information contained in noisy sample $(\tilde{\mathbf{x}}(0), \mathbf{r} \neq \mathbf{0})$ during optimization.

6.3 Extension under Cauchy Perturbation

In terms of Theorem 5, we provide a corollary that applies *risk-sensitive diffusion* to VE SDE, letting it be robust to Cauchy-corrupted samples.

Corollary 5 (Risk-sensitive VE SDE for Cauchy Noises). *For the weight function $\Omega(\mathbf{y}) = |\boldsymbol{\chi}_t(\mathbf{y})|^2$ and a Cauchy noise distribution $\rho_{\mathbf{r}}(\boldsymbol{\epsilon})$ that is specified by scales \mathbf{r} (i.e., risk vector):*

$$\rho_{\mathbf{r}}(\boldsymbol{\epsilon}) = \prod_{j=1}^D \left(\pi r_j \left(1 + \frac{\epsilon_j^2}{r_j^2} \right) \right)^{-1},$$

the minimally-unstable risk-sensitive SDE (defined by Eq. (13)) for VE SDE has a drift coefficient as $\mathbf{f}(\mathbf{r}, t) = \mathbf{0}$ and a diffusion coefficient as

$$\mathbf{g}(\mathbf{r}, t) = \mathbb{1}(\sigma(t)^2 \mathbf{1} \succeq \sigma(0)^2 \mathbf{1} + \boldsymbol{\psi}(\mathbf{r})) \sqrt{\frac{d\sigma(t)^2}{dt}},$$

where the term $\boldsymbol{\psi}(\mathbf{r})$ is defined as

$$\boldsymbol{\psi}(\mathbf{r}) = (\mathbf{r}^{-2}(\mathbf{r}^{-2})^\top + \text{diag}(5\mathbf{r}^{-4}))^{-1} (\mathbf{r}^{-1} \mathbf{1}^\top \mathbf{r}^{-1} + 2\mathbf{r}^{-2}).$$

The vector \mathbf{r} is element-wise non-negative. For $\mathbf{r} = \mathbf{0}$, the risk-sensitive SDE reduces to VE SDE, with $\mathbf{f}(\mathbf{0}, t) = \mathbf{0}, \mathbf{g}(\mathbf{0}, t) = \sqrt{d\sigma(t)^2/dt}$.

Proof. Based on Theorem 5, we aim to derive risk-sensitive SDEs for the noises sampled from a multivariate Cauchy distribution. We first suppose a noise $\boldsymbol{\epsilon} = [\epsilon_1, \epsilon_2, \dots, \epsilon_D]^\top$, with every dimension $j \in [1, D]$ being independent and following a univariate Cauchy distribution $\rho_j(\epsilon_j)$ that is parameterized by scale κ_j :

$$\rho_j(\epsilon_j) = \frac{1}{\pi \kappa_j (1 + \epsilon_j^2 / \kappa_j^2)}, \quad \phi_j(\omega_j) = \exp(-\kappa_j |\omega_j|), \quad (77)$$

where $\phi_j(\omega_j)$ is the characteristic function of distribution $\rho_j(\epsilon_j)$. Then, because random variables $\epsilon_1, \epsilon_2, \dots, \epsilon_D$ are mutually independent, their joint distribution $\rho(\boldsymbol{\epsilon})$ is equal to $\prod_{j=1}^D \rho_j(\epsilon_j)$ and we can derive its characteristic function $\phi(\boldsymbol{\omega})$ as

$$\begin{aligned} \phi(\boldsymbol{\omega}) &= \mathbb{E}_{\boldsymbol{\epsilon} \sim \rho(\boldsymbol{\epsilon})}[\exp(i\boldsymbol{\epsilon}^\top \boldsymbol{\omega})] = \int \rho(\boldsymbol{\epsilon}) \exp(i\boldsymbol{\epsilon}^\top \boldsymbol{\omega}) d\boldsymbol{\epsilon} \\ &= \prod_{j=1}^D \left(\int \rho_j(\epsilon_j) \exp(i\epsilon_j \omega_j) d\omega_j \right) = \exp(-\boldsymbol{\kappa}^\top |\boldsymbol{\omega}|), \end{aligned} \quad (78)$$

where $\boldsymbol{\kappa} = [\kappa_1, \kappa_2, \dots, \kappa_D]$. Now, we can convert Eq. (61) into the following form:

$$\begin{aligned} \left[\int \Gamma(\boldsymbol{\omega}) \omega_i^2 \omega_j^2 d\boldsymbol{\omega} \right]_{i,j \in [1,D]} \left(\bar{\mathbf{g}}(\mathbf{0}, t)^2 - \bar{\mathbf{g}}(\mathbf{r}, t)^2 \right) &= -2 \left[\int \Gamma(\boldsymbol{\omega}) \ln |\phi(\bar{\mathbf{f}}(t) \odot \boldsymbol{\omega})| \omega_i^2 d\boldsymbol{\omega} \right]_{i \in [1,D]}^\top \\ &= 2 \left[\int \Gamma(\boldsymbol{\omega}) (\bar{\mathbf{f}}(t) \odot \boldsymbol{\kappa})^\top |\boldsymbol{\omega}| \omega_i^2 d\boldsymbol{\omega} \right]_{i \in [1,D]}^\top = 2 \left[\int \Gamma(\boldsymbol{\omega}) |\omega_i| \omega_j^2 d\boldsymbol{\omega} \right]_{i,j \in [1,D]} \left(\bar{\mathbf{f}}(t) \odot \boldsymbol{\kappa} \right). \end{aligned} \quad (79)$$

We set the weight function $\Gamma(\boldsymbol{\omega})$ as the magnitude of the characteristic function $|\phi(\boldsymbol{\omega})|$ since it indicates the importance of value $\boldsymbol{\omega}$. In this regard, consider the below five integrals:

$$\begin{aligned} \int \exp(-\kappa_j |\omega_j|) d\omega_j &= \frac{2}{\kappa_j}, \quad \int \exp(-\kappa_j |\omega_j|) \omega_j^2 d\omega_j = \frac{4}{\kappa_j^3}, \quad \int \exp(-\kappa_j |\omega_j|) |\omega_j| d\omega_j = \frac{2}{\kappa_j^2}, \\ \int \exp(-\kappa_j |\omega_j|) \omega_j^4 d\omega_j &= \frac{48}{\kappa_j^5}, \quad \int \exp(-\kappa_j |\omega_j|) \omega_j^2 |\omega_j| d\omega_j = \frac{12}{\kappa_j^4}. \end{aligned} \quad (80)$$

we can solve that linear equation as

$$\bar{\mathbf{g}}(\mathbf{0}, t)^2 - \bar{\mathbf{g}}(\mathbf{r}, t)^2 = \left[\frac{1 + 5\mathbb{1}(i=j)}{\kappa_i^2 \kappa_j^2} \right]_{i,j \in [1,D]}^{-1} \left[\frac{1 + 2\mathbb{1}(i=j)}{\kappa_i \kappa_j^2} \right]_{i,j \in [1,D]} \left(\bar{\mathbf{f}}(t) \odot \boldsymbol{\kappa} \right). \quad (81)$$

For demonstration purposes, let's consider the case of $D = 1$:

$$\bar{g}(r, t)^2 = \bar{g}(0, t)^2 - \frac{1}{2} \bar{f}(t) \kappa^2. \quad (82)$$

For $D > 1$, we can only have the below form with an inverse matrix:

$$\bar{\mathbf{g}}(\mathbf{r}, t)^2 = \bar{\mathbf{g}}(\mathbf{0}, t)^2 - \bar{\mathbf{f}}(t) \odot \left((\boldsymbol{\kappa}^{-2} (\boldsymbol{\kappa}^{-2})^\top + \text{diag}(5\boldsymbol{\kappa}^{-4}))^{-1} (\boldsymbol{\kappa}^{-1} \mathbf{1}^\top \boldsymbol{\kappa}^{-1} + 2\boldsymbol{\kappa}^{-2}) \right), \quad (83)$$

where $\boldsymbol{\kappa}^{-n} = [\kappa_1^{-n}, \kappa_2^{-n}, \dots, \kappa_D^{-n}]$, $n \in \mathcal{N}^+$. \square

For risk-sensitive VE SDE under Cauchy Perturbation, the concept of stability interval does not apply, though its coefficient $\mathbf{g}(\mathbf{r}, t)$ is optimal in a sense that the instability measure $\mathcal{S}_t(\mathbf{r})$ is minimized. For optimization, one can simply set $\mathcal{T}(\mathbf{r}) = [0, T]$ and apply Algorithm 1. In Appendix C, our numerical experiments show that the risk-sensitive VE SDE are very robust for optimization with Cauchy-corrupted samples (i.e., Fig. 4).

References

- [AB21] Anastasios N Angelopoulos and Stephen Bates. A gentle introduction to conformal prediction and distribution-free uncertainty quantification. *arXiv preprint arXiv:2107.07511*, 2021. 5
- [Ahr05] Peter Ahrendt. The multivariate gaussian probability distribution. *Technical University of Denmark, Tech. Rep*, page 203, 2005. 13
- [AN07] Arthur Asuncion and David Newman. Uci machine learning repository, 2007. 34
- [And82] Brian DO Anderson. Reverse-time diffusion equation models. *Stochastic Processes and their Applications*, 12(3):313–326, 1982. 32
- [And12] William J Anderson. *Continuous-time Markov chains: An applications-oriented approach*. Springer Science & Business Media, 2012. 5
- [AYHVdS17] Ahmed M Alaa, Jinsung Yoon, Scott Hu, and Mihaela Van der Schaar. Personalized risk scoring for critical care prognosis using mixtures of gaussian processes. *IEEE Transactions on Biomedical Engineering*, 65(1):207–218, 2017. 33
- [Chu01] Kai Lai Chung. *A course in probability theory*. Academic press, 2001. 9, 10
- [CP96] Dwyane C Carmer and Lauren M Peterson. Laser radar in robotics. *Proceedings of the IEEE*, 84(2):299–320, 1996. 5
- [CSCP21] Pierre Colombo, Guillaume Staerman, Chloé Clavel, and Pablo Piantanida. Automatic text evaluation through the lens of Wasserstein barycenters. In Marie-Francine Moens, Xuanjing Huang, Lucia Specia, and Scott Wen-tau Yih, editors, *Proceedings of the 2021 Conference on Empirical Methods in Natural Language Processing*, pages 10450–10466, Online and Punta Cana, Dominican Republic, November 2021. Association for Computational Linguistics. 34
- [CY22] Hyungjin Chung and Jong Chul Ye. Score-based diffusion models for accelerated mri. *Medical image analysis*, 80:102479, 2022. 5
- [DD11] Anirban DasGupta and Anirban DasGupta. Characteristic functions and applications. *Probability for Statistics and Machine Learning: Fundamentals and Advanced Topics*, pages 293–322, 2011. 16
- [DDS⁺09] Jia Deng, Wei Dong, Richard Socher, Li-Jia Li, Kai Li, and Li Fei-Fei. Imagenet: A large-scale hierarchical image database. In *2009 IEEE conference on computer vision and pattern recognition*, pages 248–255. Ieee, 2009. 5
- [DG06] Jesse Davis and Mark Goadrich. The relationship between precision-recall and roc curves. In *Proceedings of the 23rd international conference on Machine learning*, pages 233–240, 2006. 34
- [DN21] Prafulla Dhariwal and Alexander Nichol. Diffusion models beat gans on image synthesis. *Advances in neural information processing systems*, 34:8780–8794, 2021. 1, 6, 30

- [DSD⁺24] Giannis Daras, Kulin Shah, Yuval Dagan, Aravind Gollakota, Alex Dimakis, and Adam Klivans. Ambient diffusion: Learning clean distributions from corrupted data. *Advances in Neural Information Processing Systems*, 36, 2024. 6
- [Eva12] Lawrence C Evans. *An introduction to stochastic differential equations*, volume 82. American Mathematical Soc., 2012. 10
- [GG16] Yarin Gal and Zoubin Ghahramani. Dropout as a bayesian approximation: Representing model uncertainty in deep learning. In *international conference on machine learning*, pages 1050–1059. PMLR, 2016. 5
- [GPAM⁺20] Ian Goodfellow, Jean Pouget-Abadie, Mehdi Mirza, Bing Xu, David Warde-Farley, Sherjil Ozair, Aaron Courville, and Yoshua Bengio. Generative adversarial networks. *Communications of the ACM*, 63(11):139–144, 2020. 5
- [HJA20] Jonathan Ho, Ajay Jain, and Pieter Abbeel. Denoising diffusion probabilistic models. *Advances in Neural Information Processing Systems*, 33:6840–6851, 2020. 1, 6, 9, 19, 22, 34
- [HLC21] Chin-Wei Huang, Jae Hyun Lim, and Aaron Courville. A variational perspective on diffusion-based generative models and score matching. In A. Beygelzimer, Y. Dauphin, P. Liang, and J. Wortman Vaughan, editors, *Advances in Neural Information Processing Systems*, 2021. 1
- [HRU⁺17] Martin Heusel, Hubert Ramsauer, Thomas Unterthiner, Bernhard Nessler, and Sepp Hochreiter. Gans trained by a two time-scale update rule converge to a local nash equilibrium. *Advances in neural information processing systems*, 30, 2017. 34
- [HS21] Jonathan Ho and Tim Salimans. Classifier-free diffusion guidance. In *NeurIPS 2021 Workshop on Deep Generative Models and Downstream Applications*, 2021. 6, 30
- [HZXW23] Lei Huang, Hengtong Zhang, Tingyang Xu, and Ka-Chun Wong. Mdm: Molecular diffusion model for 3d molecule generation. In *Proceedings of the AAAI Conference on Artificial Intelligence*, volume 37, pages 5105–5112, 2023. 5
- [Itô44] Kiyosi Itô. 109. stochastic integral. *Proceedings of the Imperial Academy*, 20(8):519–524, 1944. 1, 7
- [JPS⁺16] Alistair EW Johnson, Tom J Pollard, Lu Shen, Li-wei H Lehman, Mengling Feng, Mohammad Ghassemi, Benjamin Moody, Peter Szolovits, Leo Anthony Celi, and Roger G Mark. Mimic-iii, a freely accessible critical care database. *Scientific data*, 3(1):1–9, 2016. 5, 8, 33
- [KB⁺18] Youngjoo Kim, Hyochoong Bang, et al. Introduction to kalman filter and its applications. *Introduction and Implementations of the Kalman Filter*, 1:1–16, 2018. 5
- [KG17] Alex Kendall and Yarin Gal. What uncertainties do we need in bayesian deep learning for computer vision? *Advances in neural information processing systems*, 30, 2017. 5

- [KJCT12] Martti Kirkko-Jaakkola, Jussi Collin, and Jarmo Takala. Bias prediction for mems gyroscopes. *IEEE Sensors Journal*, 12(6):2157–2163, 2012. 5
- [KK14] Arbind Kumar and Jagdeep Kaur. Primer based approach for pcr amplification of high gc content gene: Mycobacterium gene as a model. *Molecular biology international*, 2014, 2014. 4
- [KNJ⁺24] Yeongmin Kim, Byeonghu Na, JoonHo Jang, Minsang Park, Dongjun Kim, Wanmo Kang, and Il chul Moon. Training unbiased diffusion models from biased dataset. In *The Twelfth International Conference on Learning Representations*, 2024. 6
- [KNS⁺19] Soheil Kolouri, Kimia Nadjahi, Umut Simsekli, Roland Badeau, and Gustavo Rohde. Generalized sliced wasserstein distances. *Advances in neural information processing systems*, 32, 2019. 34
- [KPH⁺21] Zhifeng Kong, Wei Ping, Jiaji Huang, Kexin Zhao, and Bryan Catanzaro. Diffwave: A versatile diffusion model for audio synthesis. In *International Conference on Learning Representations*, 2021. 1
- [Kra18] Steven G Krantz. *Partial differential equations and complex analysis*. CRC press, 2018. 15
- [KVJ23] Ivan Kapelyukh, Vitalis Vosylius, and Edward Johns. Dall-e-bot: Introducing web-scale diffusion models to robotics. *IEEE Robotics and Automation Letters*, 2023. 5
- [LBH15] Yann LeCun, Yoshua Bengio, and Geoffrey Hinton. Deep learning. *nature*, 521(7553):436–444, 2015. 1
- [LDB17] Martin F Laursen, Marlene D Dalgaard, and Martin I Bahl. Genomic gc-content affects the accuracy of 16s rrna gene sequencing based microbial profiling due to pcr bias. *Frontiers in microbiology*, 8:287367, 2017. 4
- [LT20] Wei-Chao Lin and Chih-Fong Tsai. Missing value imputation: a review and analysis of the literature (2006–2017). *Artificial Intelligence Review*, 53:1487–1509, 2020. 5
- [LTG⁺22] Xiang Li, John Thickstun, Ishaan Gulrajani, Percy S Liang, and Tatsunori B Hashimoto. Diffusion-lm improves controllable text generation. *Advances in Neural Information Processing Systems*, 35:4328–4343, 2022. 1
- [LvdS24] Yangming Li and Mihaela van der Schaar. On error propagation of diffusion models. In *The Twelfth International Conference on Learning Representations*, 2024. 1
- [M⁺98] David JC MacKay et al. Introduction to gaussian processes. *NATO ASI series F computer and systems sciences*, 168:133–166, 1998. 5, 8
- [NKB⁺24] Byeonghu Na, Yeongmin Kim, HeeSun Bae, Jung Hyun Lee, Se Jung Kwon, Wanmo Kang, and Il chul Moon. Label-noise robust diffusion models. In *The Twelfth International Conference on Learning Representations*, 2024. 6
- [Oks13] Bernt Oksendal. *Stochastic differential equations: an introduction with applications*. Springer Science & Business Media, 2013. 10

- [ØØ03] Bernt Øksendal and Bernt Øksendal. *Stochastic differential equations*. Springer, 2003. 14
- [OXLC23] Yidong Ouyang, Liyan Xie, Chongxuan Li, and Guang Cheng. Missdiff: Training diffusion models on tabular data with missing values. *arXiv preprint arXiv:2307.00467*, 2023. 6
- [Pet09] Leif E Peterson. K-nearest neighbor. *Scholarpedia*, 4(2):1883, 2009. 34
- [RCD19] Yulia Rubanova, Ricky TQ Chen, and David K Duvenaud. Latent ordinary differential equations for irregularly-sampled time series. *Advances in neural information processing systems*, 32, 2019. 7
- [RvdOV19] Ali Razavi, Aaron van den Oord, and Oriol Vinyals. Generating diverse high-fidelity images with vq-vae-2. In H. Wallach, H. Larochelle, A. Beygelzimer, F. d'Alché-Buc, E. Fox, and R. Garnett, editors, *Advances in Neural Information Processing Systems*, volume 32. Curran Associates, Inc., 2019. 34
- [S⁺97] Steven W Smith et al. The scientist and engineer’s guide to digital signal processing, 1997. 10
- [SB12] Daniel J Stekhoven and Peter Bühlmann. Missforest—non-parametric missing value imputation for mixed-type data. *Bioinformatics*, 28(1):112–118, 2012. 5
- [SBL⁺18] Mehdi SM Sajjadi, Olivier Bachem, Mario Lucic, Olivier Bousquet, and Sylvain Gelly. Assessing generative models via precision and recall. *Advances in neural information processing systems*, 31, 2018. 34
- [SC05] Ove Steinvall and Tomas Chevalier. Range accuracy and resolution for laser radars. In *Electro-Optical Remote Sensing*, volume 5988, pages 73–88. SPIE, 2005. 1, 5
- [SDCS23] Yang Song, Prafulla Dhariwal, Mark Chen, and Ilya Sutskever. Consistency models. In *Proceedings of the 40th International Conference on Machine Learning, ICML’23*. JMLR.org, 2023. 4
- [SDWGM15] Jascha Sohl-Dickstein, Eric Weiss, Niru Maheswaranathan, and Surya Ganguli. Deep unsupervised learning using nonequilibrium thermodynamics. In *International Conference on Machine Learning*, pages 2256–2265. PMLR, 2015. 1
- [SE19] Yang Song and Stefano Ermon. Generative modeling by estimating gradients of the data distribution. *Advances in neural information processing systems*, 32, 2019. 1, 6, 7
- [SHSL20] Chenxi Sun, Shenda Hong, Moxian Song, and Hongyan Li. A review of deep learning methods for irregularly sampled medical time series data. *arXiv preprint arXiv:2010.12493*, 2020. 5
- [SSDK⁺21] Yang Song, Jascha Sohl-Dickstein, Diederik P Kingma, Abhishek Kumar, Stefano Ermon, and Ben Poole. Score-based generative modeling through stochastic differential equations. In *International Conference on Learning Representations*, 2021. 1, 2, 4, 6, 7, 9, 19

- [SSGL23] Ajay Sridhar, Dhruv Shah, Catherine Glossop, and Sergey Levine. Nomad: Goal masked diffusion policies for navigation and exploration. In *First Workshop on Out-of-Distribution Generalization in Robotics at CoRL 2023*, 2023. 5
- [TWY17] Qijian Tang, Xiangjun Wang, and Qingping Yang. Scale factor model analysis of mems gyroscopes. *Microsystem Technologies*, 23:1215–1219, 2017. 5
- [Wei05] Sanford Weisberg. *Applied linear regression*, volume 528. John Wiley & Sons, 2005. 9
- [ZDJR23] Margaux Zaffran, Aymeric Dieuleveut, Julie Josse, and Yaniv Romano. Conformal prediction with missing values. In *International Conference on Machine Learning*, pages 40578–40604. PMLR, 2023. 5

A Risk-conditional SGM

An obvious way to adapt current SGM to the extra risk information \mathbf{r} is conditional generation [DN21]. The main drawback of conditional SGM is that it might have a biased sampling distribution. For example, suppose a regressor-guided diffusion model [DN21] is trained on a dataset composed of blurry pictures of dogs and clear pictures of cats, then the conditional model will generate very few images of dogs, given that they are associated with a higher risk than cats. In the following, we present three different implementations under this scheme.

A.1 Risk as the Variable

A naive implementation is first to let diffusion models learn the joint distribution of samples and risk vectors: $p_0(\mathbf{x}, \mathbf{r})$, and then regularize the reverse process for drawing samples of a low risk: $\mathbf{r} \approx \mathbf{0}$, from the trained model.

Risk variable. In the optimization stage, we concatenate the sample and risk vectors as $\mathbf{z}(0) = \tilde{\mathbf{x}}(0) \oplus \mathbf{r}$ in a column-wise manner, with Eq. (8) and Eq.(10) to train a vanilla diffusion model. We draw low-risk samples from the trained model at inference time through an improved backward SDE. Considering the technique of classifier guidance [DN21], we set a parameter-free regressor $-\|\cdot\|_2$: the minus square norm, which takes the last D entries of variable $\mathbf{z}_{D+1:2D}(t) := \mathbf{r}(t)$ as the input and has a derivate as $-\nabla_{\mathbf{r}(t)}\|\mathbf{r}(t)\|_2 = -\mathbf{r}(t)/\|\mathbf{r}(t)\|_2$. With this regressor, the backward process (i.e., Eq. (9)) is updated as follows:

$$\begin{aligned} d\mathbf{z}(t) &= \left(\mathbf{f}(\mathbf{z}(t), t) - g(t)^2(\nabla_{\mathbf{z}(t)} \ln p_t(\mathbf{z}(t)) - \nabla_{\mathbf{r}(t)}\|\mathbf{r}(t)\|_2) \right) + g(t)d\bar{\mathbf{w}}(t) \\ &= \left(\mathbf{f}(\mathbf{z}(t), t) - g(t)^2 \left(\nabla \ln p_t(\mathbf{z}(t)) - \frac{\mathbf{r}(t)}{\|\mathbf{r}(t)\|_2} \right) \right) + g(t)d\bar{\mathbf{w}}(t) \\ &\approx \left(\mathbf{f}(\mathbf{z}(t), t) - g(t)^2 \left(\mathbf{s}_\theta(\mathbf{z}(t), t) - \frac{\mathbf{r}(t)}{\|\mathbf{r}(t)\|_2} \right) \right) + g(t)d\bar{\mathbf{w}}(t), \end{aligned} \quad (84)$$

where some redundant parts are omitted as (\cdot) . In practice, the gradient $-\nabla_{\mathbf{r}(t)}\|\mathbf{r}(t)\|_2$ is re-scaled with a positive coefficient γ , which trades diversity for quality. Intuitively, the regressor $-\|\cdot\|_2$ gradually reduces the norm of $\mathbf{r}(t)$ as decreasing iteration t such that the final sample $\mathbf{x}(0) = \mathbf{z}_{1:D}(0)$ will be paired with low risk $\mathbf{r}(0)$.

A.2 Risk as the Conditional

Another type of implementation treats the risk vector \mathbf{r} as a generation conditional for diffusion models. Ideally, we can draw clean samples from a trained model by setting $\mathbf{r} = \mathbf{0}$.

Risk conditional. There are two types of conditional diffusion models. The easier one is classifier-free [HS21], which adds the risk vector \mathbf{r} as an input to the score-based model: $\mathbf{s}_\theta(\mathbf{x}, t, \mathbf{r})$. Eq. (8) and Eq. (10) are the same to train the new model, but the input \mathbf{r} is randomly masked with a dummy variable \emptyset to permit unconditional generation. For inference, the score function $\nabla_{\mathbf{x}(t)} \ln p_t(\mathbf{x}(t))$ in the backward SDE (i.e., Eq. (9)) is replaced with

$$(1 + \gamma)\mathbf{s}_\theta(\mathbf{x}(t), t, \mathbf{r} = \mathbf{0}) - \gamma\mathbf{s}_\theta(\mathbf{x}(t), t, \emptyset), \quad (85)$$

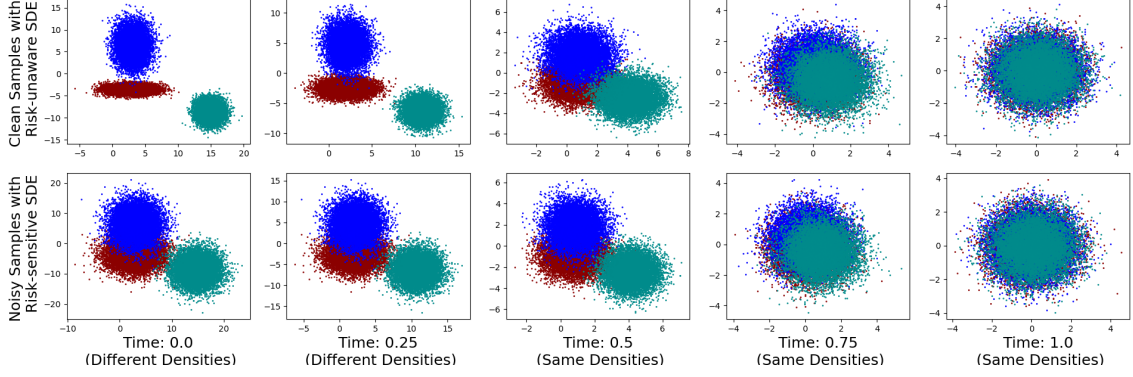


Figure 2: Comparison between the diffusion process of a standard VP SDE for clean samples (i.e., the upper 5 subfigures) and its alternative: *risk-sensitive SDE*, for Gaussian-corrupted samples (i.e., the lower 5 subfigures). With the appropriate diffusion processes, the clean and noisy samples have the same marginal densities in the *stability interval*: $t \in [0.26, 1]$.

where γ is a non-negative number that plays a similar role to the first model.

Risk regressor. The other one is just classifier-guided sampling. While the diffusion model remains the same, we separately train a regressor \mathbf{h} to predict the risk of a sample:

$$\hat{\mathbf{r}} = \ln(1 + \exp(\mathbf{h}(\mathbf{x})), \quad (86)$$

where the SoftPlus function $\exp(1 + \ln(\cdot))$ is to ensure that the final output $\hat{\mathbf{r}}$ is positive and variable \mathbf{x} is either raw sample $\tilde{\mathbf{x}}(0)$ or its noisy version $\tilde{\mathbf{x}}(t), t > 0$ (obtained by Eq. (8)). For implementation, the regressor \mathbf{h} can be any neural network and is optimized with a square loss: $\|\mathbf{r} - \hat{\mathbf{r}}\|_2^2$. To have a scalar outcome, we wrap the regressor as $-\sum_{i=1}^D \ln(1 + \exp(h_i(\mathbf{x})))$, with expansion $\mathbf{h}(\mathbf{x}) = [h_1(\mathbf{x}), h_2(\mathbf{x}), \dots, h_D(\mathbf{x})]^\top$ and derivative

$$\nabla_{\mathbf{x}} \left(-\sum_{i=1}^D \ln(1 + \exp(h_i(\mathbf{x}))) \right) = -\left[\sum_{i=1}^D \sigma(h_i(\mathbf{x})) \frac{\partial h_i(\mathbf{x})}{\partial x_1}, \dots, \sum_{i=1}^D \sigma(h_i(\mathbf{x})) \frac{\partial h_i(\mathbf{x})}{\partial x_D} \right]^\top, \quad (87)$$

where σ is the Sigmoid function. Similar to our first model, we apply this derivative to regularize the backward process of a trained diffusion model as

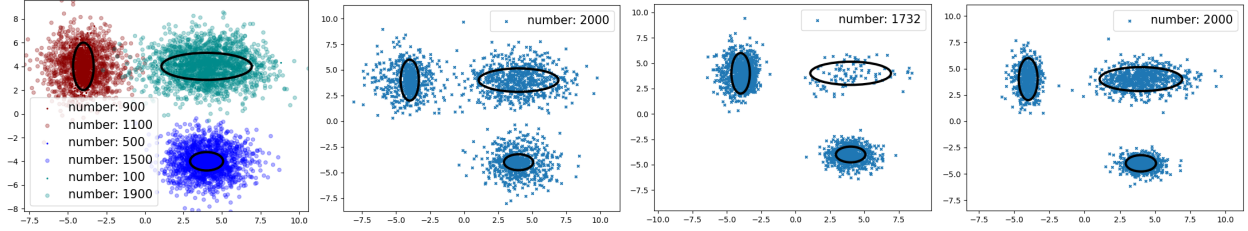
$$d\mathbf{x}(t) \approx (\mathbf{f}(\mathbf{x}(t), t) - g(t)^2(\mathbf{s}\boldsymbol{\theta}(\mathbf{x}(t), t) - \gamma \nabla_{\mathbf{x}} \left(-\sum_{i=1}^D \ln(\cdot) \right)) + g(t)d\bar{\mathbf{w}}(t), \quad (88)$$

where $\gamma \in \mathbb{R}^+ \cup \{0\}$ is non-negative.

B Backward Risk-sensitive SDE

Although the backward risk-sensitive SDE is not necessary for our method and theorems, we still provide it for reference. Let a risk-sensitive SDE be of the form as

$$d\mathbf{x}(t) = (\mathbf{f}(t) \odot \mathbf{x}(t))dt + \text{diag}(\mathbf{g}(\mathbf{r}, t))d\mathbf{w}(t), \quad (88)$$



(a) Training data, with part (b) Samples drawn from a (c) Samples drawn from (d) Samples generated from
of Gaussian-corrup- standard diffusion model. a risk-conditional diffusion our proposed model.
ples. model.

Figure 3: Comparison of *risk-sensitive VP SDE* and baselines on a Gaussian mixture (Fig. 3(a), three-sigma regions as ellipses), with Gaussian noise polluting some samples (depicted larger and in lighter color). Our model (Fig. 3(d)) successfully samples within the three-sigma ellipses, while the standard diffusion model’s samples (Fig. 3(b)) typically fall out of them, and conditional generation leads to an unbalanced distribution, with fewer samples (Fig. 3(c)) on the more noisy upper right mixture component.

where both coefficient functions $\mathbf{f}(t), \mathbf{g}(\mathbf{r}, t)$ are everywhere continuous with right derivatives. According to [And82], we can get the corresponding backward SDE as

$$\begin{aligned} d\mathbf{x} &= \left(\mathbf{f}(t) \odot \mathbf{x}(t) - \nabla_{\mathbf{x}} \cdot \text{diag}(\mathbf{g}(\mathbf{r}, t)^2) - \text{diag}(\mathbf{g}(\mathbf{r}, t)^2) \nabla_{\mathbf{x}} \ln p_t(\mathbf{x} | \mathbf{r}) \right) dt + \text{diag}(\mathbf{g}(\mathbf{r}, t)) d\bar{\mathbf{w}}(t) \\ &= \left(\mathbf{f}(t) \odot \mathbf{x}(t) - \mathbf{g}(\mathbf{r}, t)^2 \odot \nabla_{\mathbf{x}} \ln p_t(\mathbf{x} | \mathbf{r}) \right) dt + \mathbf{g}(\mathbf{r}, t) \odot d\bar{\mathbf{w}}(t). \end{aligned} \quad (88)$$

While $\mathbf{g}(\mathbf{r}, t) = \mathbf{0}$ is possible for $t \in \{t \in [1, T] \mid \bar{\mathbf{g}}(\mathbf{0}, t)^2 - \bar{\mathbf{f}}(\mathbf{r}, t)^2 \odot \tilde{\mathbf{r}}^2 \neq \bar{\mathbf{g}}(\mathbf{r}, t)^2\}$, our above conclusion still applies and the backward SDE is the same as the forward one in that case.

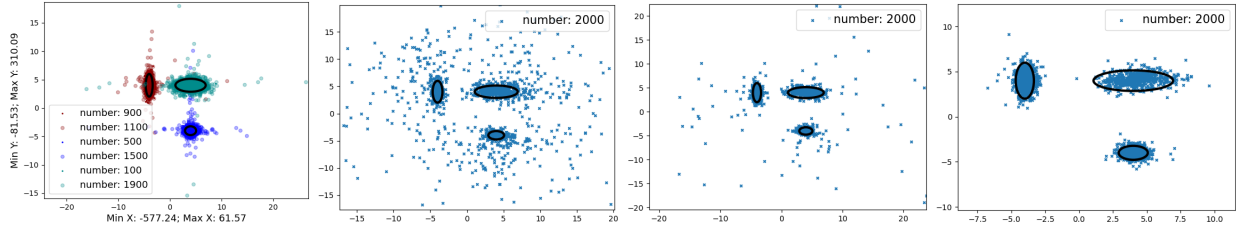
C Numerical Experiments

In this section, we provide two types of empirical results: one is to confirm the validity of our theorems in practice and the other is to apply them to real-world datasets.

C.1 Proof-of-concept Experiments

Existence of stability interval. With $T = 1, \beta(t) = 0.1 + 19.9t$, Fig. 2 shows an experiment, where VP SDE runs for clean samples $(\mathbf{x}(0), \mathbf{r} = \mathbf{0})$ while its risk-sensitive SDE (i.e., Corollary 4) operates on Gaussian-corruped samples $(\tilde{\mathbf{x}}(0), \mathbf{r} = \mathbf{1})$. We can see that the clean and noisy samples follow the same distributions for step t in the stability interval $\mathcal{T}(\mathbf{r}) = [0.26, 1]$. This experiment verifies that Theorem 3 is effective in practice.

Risk-sensitive VP SDE under Gaussian perturbation. Fig. 3 shows how a risk-conditional diffusion model compares to ours (see Example 4, and Algorithms 1 and 2) when applied to a dataset (Fig. 3(a)) sampled from a Gaussian mixture, with part of samples corrupted by Gaussian noises. The conditional model underrepresents (Fig. 3(c)) the upper-right component at low-risk generation because it contains many more (i.e., 95%) noisy samples than other components. Instead, our



(a) Training samples, with (b) Samples generated by a (c) Samples generated by (d) Samples generated by some corrupted by Cauchy standard diffusion model. a risk-conditional diffusion our proposed model. noises. model.

Figure 4: Comparison between the baselines and our model (i.e., *risk-sensitive VE SDE*) on a dataset (Fig. 4(a)) that is sampled from a Gaussian mixture, with part of the samples corrupted with a Cauchy perturbation. While our model (Fig. 4(d)) recovers the distribution of clean samples, both standard (Fig. 4(c)) and conditional models (Fig. 4(b)) incorrectly produce many outliers.

model’ (Fig. 3(d)) generated samples are mostly unbiased, with no preference for a specific mixture component. This experiment confirms the weakness of the risk-conditional baseline and verifies that our proposed model is more robust in practice.

Risk-sensitive VP SDE under Cauchy perturbation. With heavy tails, Cauchy distributions can usually distort a clean sample far away, exhibiting a distinct behavior from Gaussian noises. Fig. 4 shows an experiment where risk-sensitive VE SDE a Gaussian-mixture data as in Fig. 3(a) but with Cauchy noises corrupting samples. While risk-sensitive SDE cannot achieve *perturbation stability* in this case, our model still nicely recovers the distribution of clean samples and is robust to outliers (Fig. 4(d)). In contrast, the generated distributions of both standard (Fig. 4(c)) and conditional models (Fig. 4(b)) are seriously biased by outliers. This experiment highlights the flexibility of risk-sensitive SDEs and indicates that *risk-sensitive SDE* can still be very effective under *minimally instability*.

C.2 Application Experiments

While the *risk-sensitive SDE* has a solid theoretical foundation and is shown to be effective in synthetic experiments, we now assess the Gaussian variant (Example 4) on two relevant tasks across several real-world datasets to attest its effectiveness.

Irregular time series. As depicted in Fig. 1, irregular time series are characterized by irregularly spaced observations. To reshape such data into proper training samples for diffusion models, we must first interpolate missing observations, resulting in noisy training samples. For this scenario, we adopt 2 medical time series datasets: MIMIC-III [JPS⁺16] and WARDS [AYHVdS17]. For every time series in a dataset, we extract the observations of the first 48 hours and select their top 5 features with the highest variance, leading to a 240-dimensional vector. For the missing features, we apply the Gaussian process to interpolate them and estimate the standard deviations, which are treated as the risk information. Since WARDS is very noisy, we also set a tiny probability 0.01 that the *stability interval* is forced to be $[0, T]$ to accelerate convergence near time $t = 0$.

Model	Irregular Time Series		Tabular Data with Missing Values		
	MIMIC-III	WARDS	Abalone	Telemonitoring	Mushroom
Standard VE SDE	10.083	9.116	1.032	8.140	5.196
VE SDE w/ Risk Regressor	7.721	7.923	0.797	4.983	4.636
VE SDE w/ Risk Variable	6.549	7.314	0.853	5.161	4.970
VE SDE w/ Risk Conditional	5.926	5.951	0.612	3.159	4.101
Our Model: Risk-sensitive VE SDE	1.865	2.513	0.089	1.582	0.713
Standard VP SDE	9.135	8.765	0.925	9.935	6.238
VP SDE w/ Risk Regressor	7.981	7.832	0.732	4.197	5.327
VP SDE w/ Risk Variable	6.723	7.515	0.899	5.159	5.583
VP SDE w/ Risk Conditional	5.637	6.292	0.585	3.785	4.850
Our Model: Risk-sensitive VP SDE	1.625	2.584	0.077	1.462	0.852

Table 1: Wasserstein distances of different models on 5 datasets across 2 tasks.

Tabular data with missing values. Tabular data is naturally composed of fixed-dimensional vectors, though they usually contain missing values, and imputations of those values introduce noise. For this scenario, we adopt 3 UCI datasets [AN07]: Abalone, Telemonitoring, and Mushroom. Since these datasets are initially complete, we force the missingness by randomly masking 5% of the entries in each dataset. For an example with missing values, we first apply the k-nearest neighbors (KNN) algorithm [Pet09] to find the 10 closest samples. Then, we impute the missing value with their median and treat their absolute median deviation as the risk.

Experiment setup and results. Following common practices [HJA20], we adopt the commonly used Wasserstein Distance [HRU⁺17, KNS⁺19, CSCP21] to evaluate the generative models, which measures the discrepancy of two distributions. For baselines, we adopt two standard diffusion models (VE SDE and VP SDE) and three risk-conditional models (details in Appendix A). In Table 1, we can see that our models significantly outperform all baselines regardless of the backbone model and the dataset. For example, with VE SDE as the backbone, our model has Wasserstein distances lower than Risk Conditional by 1.577 on the Telemonitoring dataset and 4.063 on MIMIC-III.

We also depict the PRD curves [SBL⁺18, RvdOV19] of our model and two baselines on the Telemonitoring dataset. The PRD curve is similar to the precision-recall curve [DG06] used in testing classification models: the curves that locate more at the upper right corner indicate better performances. From Fig. 5, we can see that our model consistently achieves better recall scores than the baselines at identical precision scores. Plus, the PRD curve of our model is very close to the upper right corner, indicating the generation distribution of our model is almost consistent with the distribution of clean samples.

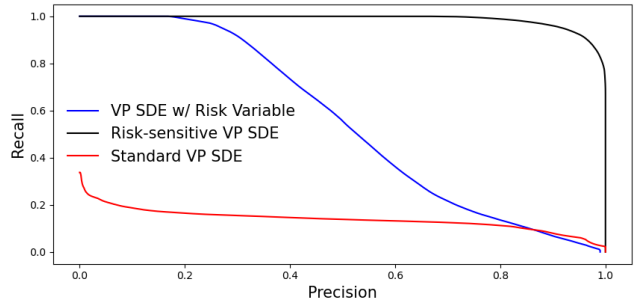


Figure 5: PRD curves (i.e., precision and recall scores) of our model and baselines on Telemonitoring dataset.